

UNCLASSIFIED

AD NUMBER
AD829131
NEW LIMITATION CHANGE
TO Approved for public release, distribution unlimited
FROM Distribution authorized to U.S. Gov't. agencies and their contractors; Critical Technology; 02 FEB 1968. Other requests shall be referred to Naval Ordnance Laboratory, White Oak, MD 20910.
AUTHORITY
NSWC ltr dtd 7 Oct 1974

THIS PAGE IS UNCLASSIFIED

AD829131

NOLTR 67-169

THE RESPONSE OF NITROGUANIDINE TO
A STRONG SHOCK

NOL

2 FEBRUARY 1968

D D C
RECEIVED
APR 1 1968
B

UNITED STATES NAVAL ORDNANCE LABORATORY, WHITE OAK, MARYLAND

NOLTR 67-169

This document is subject to special
export controls and each transmittal
to foreign governments may be made
only with prior approval of NOL.

NOLTR 67-169

THE RESPONSE OF
NITROGUANIDINE TO A STRONG SHOCK

By

Donna Price and A. R. Clairmont, Jr.

ABSTRACT: In its range of detonability, nitroguanidine (NQ) behaves as a Group 1 explosive. In addition, it exhibits failure at the high TMD ($\geq 94\%$ at 5.08 cm diam) as well as the more common failure at a lower critical density. The high bulk density (HBD) form of NQ exhibits a critical diameter about three times that of the low bulk density form. This fact aided in studying the subcritical region of NQ (HBD) where a strong shock produces a subdetonation, supersonic, constant velocity front. This pseudo-detonation or LVD had failure characteristics similar to the detonability limits of Group 2 materials. That trend, the power of the LVD reactions, and the dimensions of the various gap tests can be combined to explain (1) a hump in the curve 50% pressure vs % TMD obtained for NQ(HBD) in the gap test and (2) a reversal in apparent shock sensitivity rating of NQ(HBD) and NQ(LBD) when tested on the large- and small-scale gap tests.

Approved by:

Carl Boyars
ADVANCED CHEMISTRY DIVISION
CHEMISTRY RESEARCH DEPARTMENT
U.S. NAVAL ORDNANCE LABORATORY
White Oak, Silver Spring, Maryland

NOLTR 67-169

2 February 1968

THE RESPONSE OF NITROGUANIDINE TO A STRONG SHOCK

This work was carried out under ORDTASK 033 102 F009 06 01 Prob 001 and MAT 03L 000 R011 01 01. Its results are particularly useful in the interpretation of gap test results as shock sensitivity of the test explosive, and in providing information about pseudo-detonation (LVD) in granular charges.

E. F. SCHREIFER
Captain, USN
Commander

Albert Lightbody
ALBERT LIGHTBODY
By direction

TABLE OF CONTENTS

	Page
INTRODUCTION	1
EXPERIMENTAL	2
Nitroguanidine	2
Charge Preparation	2
Setup and Instrumentation	3
Records	3
RESULTS AND DISCUSSION	5
Ideal Detonation Velocity.	5
NQ (LBD)	10
NQ (HBD)	13
a. Detonation	13
b. Pseudo Detonation	20
c. Effect of Particle Size	29
Shock Sensitivity.	30
SUMMARY	37
REFERENCES	39
APPENDIX A, Additional Information on the Lots of NQ Used	41
APPENDIX B, Experimental Conditions for the Shots. . . .	46

ILLUSTRATIONS

Figure	Title	Page
1	Smear Camera Record of Detonation.	4
2	Smear Camera Record of LVD	4
3	Comparison of Recent Experimental Values with Ideal Curve for NQ	8
4	Comparison of Detonation Behavior of NQ (LBD) with Ideal Curve	12

ILLUSTRATIONS (Cont'd)

Figure	Title	Page
5	Diameter Effect at $\rho_0 = 1.514$ g/cc for NQ (LBD)	14
6	Section of Limit Curve for NQ (HBD) X547	14
7	Comparison of Limit Curves for Coarse TNT and NQ (LBD)	16
8	Detonation Behavior of NQ (HBD), X530	19
9	Limit Curve for Detonation of NQ (HBD), X530	22
10	Pseudo Detonation (LVD) Behavior of NQ (HBD), X530	23
11	Comparison of Diameter Dependence of LVD in Tetryl and NQ (X530)	28
12	Limit Curve for Pseudo Detonation of NQ (HBD), X530	28
13	Shock Sensitivity Curves for High and Low Bulk Density NQ	35
14	Effect of Grinding NQ (HBD) on Its Shock Sensitivity	35
A1-A3	Photomicrographs of NQ, X588	43-45

TABLES

Table	Title	Page
1	Comparison of Recent Data with Ideal Curve D_1 vs ρ_0 For NQ.	6
2	Computed Values for NQ at $\rho_0 = 0.01$ g/cc	9
3	Detonation Velocity Data for NQ (LBD) X547	10a
4	Diameter Effect at $\rho_0 = 1.514$ g/cc for NQ (LBD) X547	11
5	Detonability Limit Data For NQ (LBD) X547	13
6	Constant Velocity Data For NQ (HBD) X530	17-18
7	Lack of Diameter Effect on D of NQ (HBD)	15
8	Critical Data for Detonation of NQ (HBD) X530	20
9	Limit Date for Pseudo Detonation of NQ (HBD)	26
10	Data from NQ's X530, X588, and X589	31
11	Previous Shock Sensitivity Tests on NQ	33
12	Most Recent Shock Sensitivity Tests on NQ.	36

NOLTR 67-169

THE RESPONSE OF
NITROGUANIDINE TO A STRONG SHOCK

Donna Price and A. R. Clairmont, Jr.

INTRODUCTION

In the course of comparing the shock sensitivity to detonation of a number of explosives, it was found that the high bulk density (HBD) form of nitroguanidine (NQ) failed to detonate in the small scale gap test.¹ Moreover, its apparent power in that test decreased with increasing loading density. This suggested the possibility that NQ might belong to Group 2 explosives typified by ammonium perchlorate.² Members of this group differ from TNT-like explosives (Group 1) in exhibiting a limit curve of increasing critical diameter with increasing critical density. As a result of this limit behavior, the typical detonation velocity (D) vs loading density (ρ_0) curve also differs from that of TNT-like materials in being non-linear and in exhibiting a maximum in D.

The purpose of the present study was to determine whether NQ is a Group 2 explosive. The study showed clearly that it is not, and also produced interesting new information about differences in behavior (detonation, detonability, and sensitivity) between the low bulk density (LBD) NQ and NQ (HBD). In particular, it provided a much more detailed picture of pseudo-detonation (or "low velocity detonation") in granular explosives than is available in the literature.

EXPERIMENTAL

Nitroguanidine

All samples of NQ, $H_2N \cdot C(NNO_2) \cdot NH_2$ were supplied by NOS, Indian Head, Md. The NQ (LBD) was manufactured by North American Cyanamid, Niagara Falls, Ontario and satisfies the military specification MIL-N-494A; its nitroguanidine content is 99.5% or greater. This material is in the form of needle-like, and frequently hollow, crystals with diameter of 5 to 10 μ and length of 60-100 μ . Only one lot of NQ (LBD) was used and that was designated X547.

The NQ (HBD) was prepared at NOS from NQ (LBD). The preparation involves precipitation under controlled conditions and in the presence of a small amount of colloiddally active material.³ The particles are chunky cylinders of l/d of about 4. The average length is reported as about 20 μ although particles of up to 200 μ have been observed in the present work. The pour-density is about 0.7 g/cc as contrasted to less than 0.2 g/cc for NQ (LBD). Two lots of NQ (HBD) were used; they were designated X530 and X589 and their sieve analyses are given in Appendix A.

The presence of the colloidng agent makes it difficult to grind the NQ (HBD). Nevertheless, NOS was successful in grinding X589 to obtain a material in which 50-60% (by number) of the particles are under 10 μ in dimensions. This lot was designated X588 and its sieve analysis and photomicrographs are also given in Appendix A.

Charge Preparation

For charge preparation, the NQ was dried at 50°C for 4 or more hours and then pressed to the required density, as shown in the tables. The lowest density charges were hand packed in cellulose acetate envelopes. The highest charge density for NQ (LBD) was 1.627 g/cc obtained in the isostatic press. NQ (HBD) can be pressed to at least 1.70 g/cc. The crystal density is 1.78 g/cc.

Cylindrical granular charges, 20.32 cm long, were prepared over the range of 1.27 to 7.62 cm in diameter. Preparation and procedures were comparable to those used in the ammonium perchlorate study.⁴

Set-up and Instrumentation

The experimental set-up of the previous work⁴ was also used here. Two inch long boosters (pentolite or tetryl) of the same diameter as the test charge were used for initiation, and a one-inch pellet of the same explosive was frequently placed as a witness at the end of the charge.

A 70 mm smear camera was used at a writing speed of 1 to 3 mm/ μ sec to follow the luminosity (or flasher enhanced luminosity) of the shock induced reaction. Film, flasher, length of charge observed, and writing speed for the photographs of each shot are tabulated in Appendix B.

Records

The records were reduced and interpreted by the methods described previously.⁴ The maximum error estimated for reading records of the lowest resolution is 1.5% in the detonation velocity. In the 14 sets of data which include replications, the average precision is 0.8%, but this value includes seven sets of low density charges (hand packed or hydrostatically pressed) for which the larger deviations (1.0 to 1.7%) most probable reflect non-uniformity of the charge, i.e., error in the effective value of ρ_0 .

The photographic records were of excellent quality and are illustrated by Figs. 1 and 2 typical of high and low velocities, respectively.

It should be mentioned that all velocity measurements will be somewhat high because a non-planar shock wave was used in the initiation. For D values comparable to that of the booster



FIG. 1 SMEAR CAMERA RECORD OF DETONATION (SHOT 279 OF NQ X530) AT $\rho_0 = 1.30$ g/cc AND $d = 5.08$ cm. LENGTH OF CHARGE OBSERVED 15.2 cm; WRITING SPEED 2 mm/ μ sec; NO FLASHER USED, MEASURED D 6.51 mm/ μ sec.)

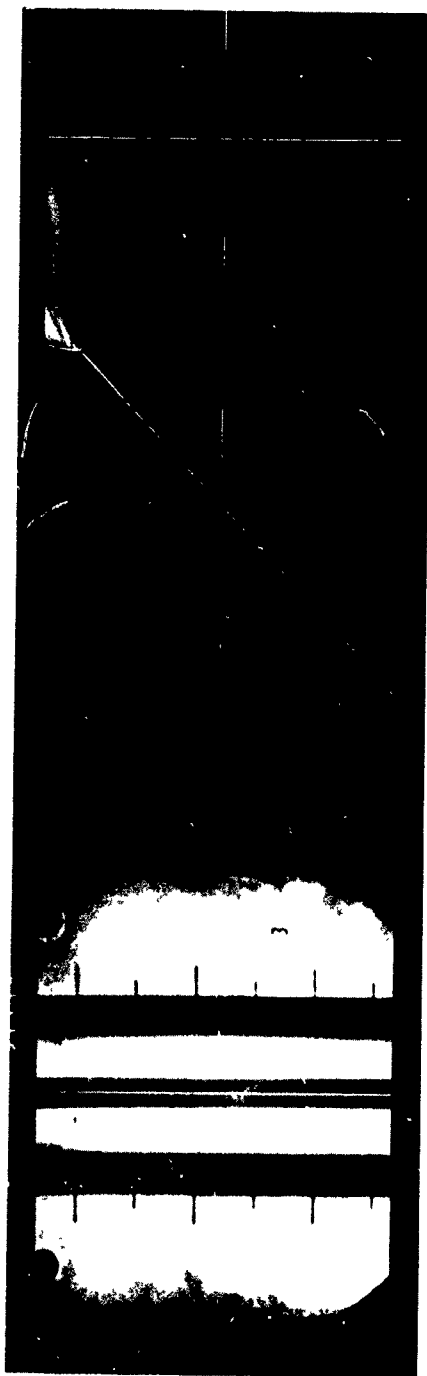


FIG. 2 SMEAR CAMERA RECORD OF LVD (SHOT 26) F NQ X530 AT $\rho_0 = 1.00$ g/cc AND $d = 2.54$ cm. LENGTH OF CHARGE OBSERVED 6.35 cm; WRITING SPEED 2 mm/ μ sec; CELLULOSE ACETATE FLASHER. MEASURED LVD OF 2.5 mm/ μ sec.)

(7.2 mm/ μ sec), this error varies from less than 0.2% at $d = 2.5$ cm to 1.5% at $d = 7.6$ cm.⁵ For lower D values, the error is less. No correction has been made for this effect, but it can be estimated whenever the size of the correction seems significant.

RESULTS AND DISCUSSION

Ideal Detonation Velocity

It is not necessary for the objectives of this work to investigate the validity of the currently accepted infinite diameter curve, D_1 vs ρ_0 , for NQ. Nevertheless, we must use the curve for reference and it seems worthwhile to see how well it fits recent data at relatively high and relatively low ρ_0 .

NQ (LBD) cannot be easily compressed to very low porosities. However, NQ (HBD), which has been available in commercial quantities for more than ten years³, can be compressed to at least 95.5% TMD and probably higher. Materials like RDX and PETN can be detonated as single crystals, i.e., at 100% TMD, but NQ at 1.70 g/cc (95.5% TMD) cannot be detonated as a 5.08 cm diameter core in a 1.27 cm thick steel tube.⁶ There are consequently no data in the older literature for D measurements at high ρ_0 .

It is not porosity alone which accounts for this detonability phenomenon because 90/10 mixtures of NQ/RDX are detonable at 95% TMD in 5.08 cm diameter, unconfined charges.^{6*} From the known ideal curve for RDX⁷ and the simple additivity principle, the D value for pure NQ at this porosity can be calculated from that measured for the mixture. The two highest density data points of Table 1 and Fig. 3 were obtained in this manner.

* It is not necessary that the material added be a more shock sensitive material. Ref. (6) also reports detonation of unconfined, 5.08 cm diameter NQ/AP, 69/31, at 96.8% TMD, a porosity at which neither component can be detonated alone. It is quite possible that an inert solid diluent would also increase detonability at low porosities.

TABLE 1
COMPARISON OF RECENT DATA WITH IDEAL CURVE* D_1 VS ρ_0 FOR NQ

Loading Density ρ_0 g/cc	Charge diam d cm	Detonation Velocity, D mm/ μ sec	Comment
1.698	5.08	8.31	Computed from Ref (6) values for NQ/RDX, 90/10, at ca. 95% TMD. Simple additivity rule used. From present work, diameter effect negligible here.
1.678	5.08	8.19	
1.620	3.8-5.1	7.98	
1.55	Unknown	7.65	Present work, Table 7, average of six values ($\sigma = 0.032$); no detectable diameter effect.
1.514	Extrapolated	7.54	Ref (9). Present work indicates very small diam. effect at this density.
1.50	Unknown	7.45	Present work, Table 4; very small diameter effect.
0.50	7 to 10	3.23	Ref (9). Same comment as for 1.55 g/cc change.
0.40	7 to 10	3.15	Ref (10)
0.30	7 to 10	2.80	Ref (10)
0.276	5.08	2.56	Ref (11) Possibly low because of diameter effect
0.18	7 to 10	2.55	Ref (12) Required 15 cm run to stabilize
0.12	>5	2.12	Ref (11)

* D_1 (mm/ μ sec) = 1.44 + 4.015 ρ_0 , Ref (8)

Two sets of data in the present work were appropriate for extrapolation to D_1 (or for averaging at the higher density of 1.62 g/cc where the diameter effect cannot be detected). One point was obtained with NQ (HBD); the second, with NQ (LBD). Both fall on the ideal curve of Fig. 3. The other high density data are from the Army Manual as indicated in Table 1.

Table 1 and Fig. 3 also contain data for the very low density range (0.12-0.50 g/cc) which can be attained because of the needle like crystals of NQ (LBD). There has been a recent interest in taking advantage of the low bulk density of this material to prepare charges exhibiting a correspondingly low detonation pressure. New low density data are available as a result.

Although the data from the very porous charges do not fall as close to the ideal curve as those at the higher densities, they lie as close to it as might be expected in view of the difficulty of controlling the uniformity of the very porous charges. However, the actual curve must diverge somewhat from the linear curve at low densities if the experimental data are to join smoothly with the value computed for $\rho_0 = 0.01$ g/cc. [The detonation parameters for $\rho_0 \approx 0$ were computed by H. Hurwitz on the Ruby code with the ideal gas law used as the equation of state for the detonation products. Results are shown in Table 2. At $\rho_0 = 0.01$ g/cc, $P_j = 187$ bars and $T_j = 2602^\circ\text{K}$. The low pressure and high temperature indicate that the ideal gas law is applicable.] Divergence of the curve is shown as the dashed line in Fig. 3. According to this, the currently accepted D_1 vs ρ_0 curve for NQ⁸

$$D_1 \text{ (mm/}\mu\text{sec)} = 1.44 + 4.015\rho_0 \quad (1)$$

holds down to $\rho_0 \sim 0.3$ g/cc. At lower densities, it diverges to a value of D_1 ($\rho_0 = 0.01$ g/cc) = 2.05 mm/ μ sec.

Stesik and Shvedova¹³ first made use of such a computation ($\rho_0 \sim 0.01$ g/cc) in studying nitrocellulose (NC), another explosive in a physical form suitable for preparing charges of very low density.

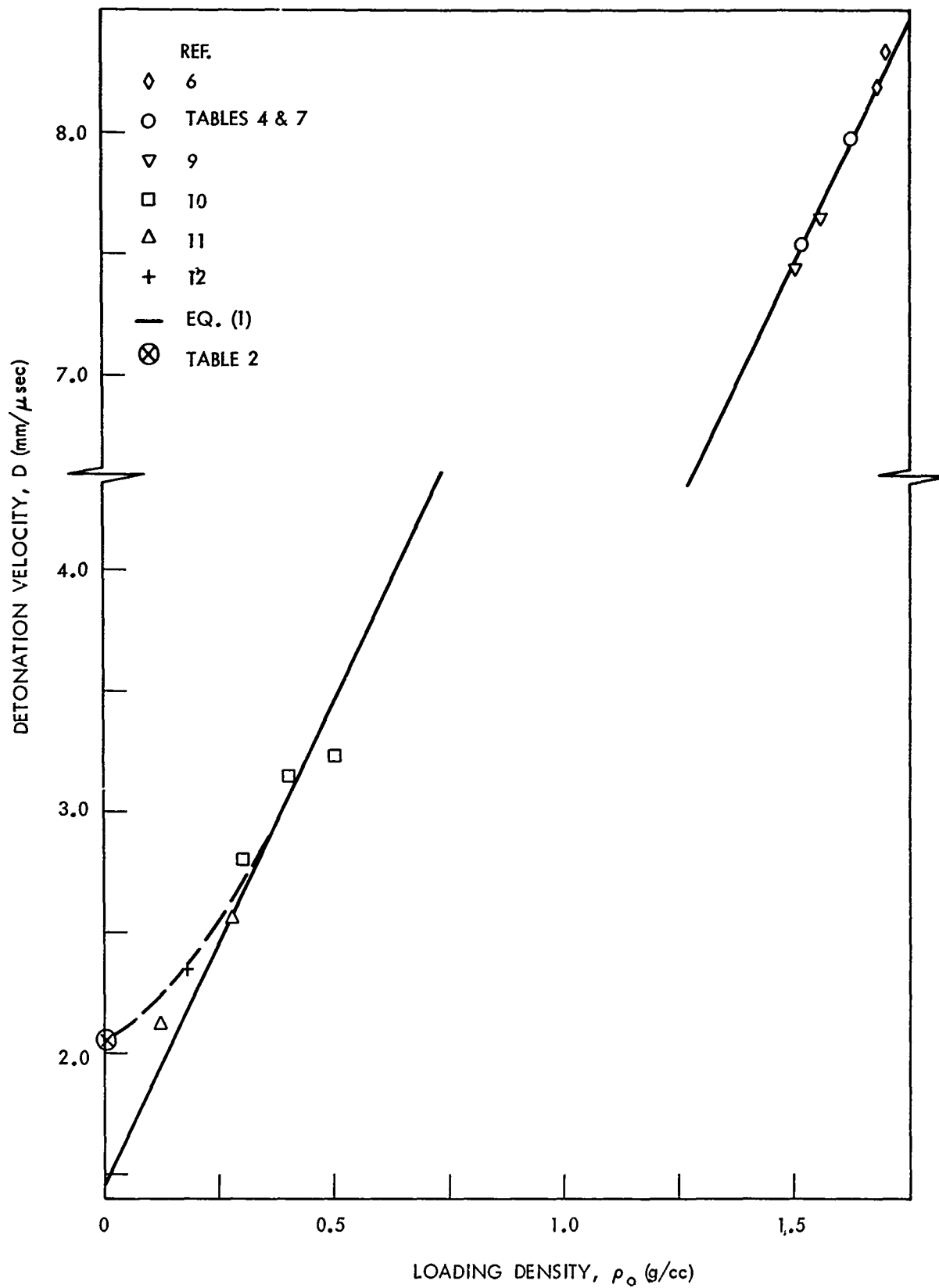


FIG. 3 COMPARISON OF RECENT EXPERIMENTAL VALUES WITH IDEAL CURVE FOR NQ

TABLE 2

COMPUTED* VALUES FOR NQ AT $\rho_0 = 0.01$ g/cc

<u>C-J Values</u>	
Velocity	2.048 mm/ μ sec
Pressure	186.7 bars
Temperature	2602 ^o K
Density	0.01795 g/cc
Gamma	1.258
Total gas	48.08 moles/1000g H.E.

<u>Detonation Products</u> (moles/1000g H.E.)	
CO	8.604
CO ₂	1.005
H	0.006
H ₂	10.585
H ₂ O	8.591
N ₂	19.215
NH ₃	0.004
OH	0.012
C (s)	0

Negligible (≤ 0.003 moles/1000g H.E.) concentration found for C(g), CH₄, N, N₂O, NO, O, and O₂.

*Ruby code with ideal gas law as equation of state for products.

Their most porous charge of NC was 0.13 g/cc and their D vs ρ_0 curve for NC is very similar to that obtained here for NQ. Moreover, they computed low density values for TNT, tetryl, picric acid, RDX, and PETN, all materials difficult to prepare at densities less than 0.5 g/cc. The computed detonation velocity values were either close to the intercept ($\rho_0 = 0$) values or well above them, as is the case for NQ. E.g., computed values for TNT, RDX, and PETN were 1.996, 2.371, and 2.194 mm/ μ sec, respectively, whereas intercept values are 1.873, 2.532, and 1.550 mm/ μ sec.

NQ (LBD)

Table 3 contains the detonation velocity measurements made on the low bulk density NQ as a function of diameter and loading density. These values (or their averages, when given in Table 3) are plotted in Fig. 4. It is evident that the diameter effect is small for this material, but that it is larger at low ρ_0 than at high. In other words the higher density data are practically on the Eq(1) curve; the lower density data, below it. Since this is the case, it is reasonable to use the slope of the ideal curve to make small corrections in the high ρ_0 data for small variations in ρ_0 . Table 4 contains the D vs d data, at $\rho_0 = 1.514$ to 1.524 g/cc of Table 3, so corrected to $\rho_0 = 1.514$ g/cc; the corrected data are plotted in Fig. 5.

(page 10a follows)

TABLE 3
 DETONATION VELOCITY DATA FOR NQ (LBD) X547

ρ_0 (g/cc)	Detonation (Shock) Velocity mm/ μ sec	Shot No.	ρ_0 (g/cc)	Detonation (Shock) Velocity mm/ μ sec	Fade-out distance, diameters	Shot No.
$\bar{d} = 3.810$ cm; (λ/d) = 5.3			$\bar{d} = 1.905$ cm; (λ/d) = 10.7			
0.477h	3.122	77	1.5141	7.440	-	138
0.442h	3.024	78 ^a	$\bar{d} = 1.588$ cm; (λ/d) = 12.8			
0.437h	2.966	79 ^a	0.604h	3.417	-	241
0.902H	4.697	102 ^b	1.2111	5.722	-	184
0.902H	4.848	103 ^b	1.5171	7.452	-	159
1.3891	7.070	105 ^c	$\bar{d} = 1.429$ cm; (λ/d) = 14.2			
1.3891	7.074	106 ^c	1.1991	F(4.46)	5.7	213
1.3891	7.143	107 ^c	1.2161	F(4.51)	4.5	215
$\bar{d} = 3.653$ cm; (λ/d) = 5.6			1.5241	7.403	-	162
1.6271	7.932	80 ^d	$\bar{d} = 1.270$ cm; (λ/d) = 16.0			
1.6271	8.106	81 ^d	1.1921	F(3.14)	3.3	175
$\bar{d} = 2.540$ cm; (λ/d) = 8.0			1.1921	F(2.59)	4.0*	176
0.558h	3.233	240	1.3201	F(5.14)	4.3	214
0.999H	5.012	422A**	1.3211	F(5.64)	5.4	216
1.1851	6.103	242	1.5191	F(7.05)	2.0	157
1.5151	7.489	133	1.5211	-	13.0*	163

Averaged values of ρ_0 and D, respectively:
 a. 0.44, 3.00(2); b. 0.90, 4.77(2); c. 1.39, 7.10(3); d. 1.63, 8.02(2).
 Symbols: F failed; h handpacked; H hydraulic press; I isostatic press.
 * Stronger booster
 ** Initiated by small booster (tetryl wafer of 1.27 cm diam x 0.635cm thick).
 Detonator alone failed to initiate a duplicate charge.

TABLE 4
 DIAMETER EFFECT AT $\rho_0 = 1.514$ g/cc for NQ (LBD) X547

<u>d</u> <u>cm</u>	<u>D*</u> <u>mm/μsec</u>	<u>10d⁻¹</u> <u>cm⁻¹</u>
∞	7.54**	0
2.540	7.485	3.937
1.905	7.440	5.249
1.588	7.440	6.297
1.429	7.363	6.998
1.270	F	7.874

*Data from previous table corrected to present density by Eq (1)
 **By extrapolation

Fig. 5 shows that the diameter effect at this density (85% TMD) is very small. The velocity at $d = 2.54$ cm is only 0.06 mm/μsec lower than that at $d = \infty$. The extrapolated value, $D_1 = 7.54$ mm/μsec, compares well with the Eq(1) value of 7.52 mm/μsec.

A few series of Table 3 were carried to the failure limit; those that were are summarized in Table 5, and the failure curve is illustrated in Fig. 6. This is typical Group 1 behavior for which the critical diameter increases with decreasing critical density. Fig. 7 compares the limit curve of NQ (LBD) with that of a coarse TNT.¹⁴ Although the trends are the same, the critical diameter of the NQ is 2 to 3 times that of the coarse TNT at the same %TMD.

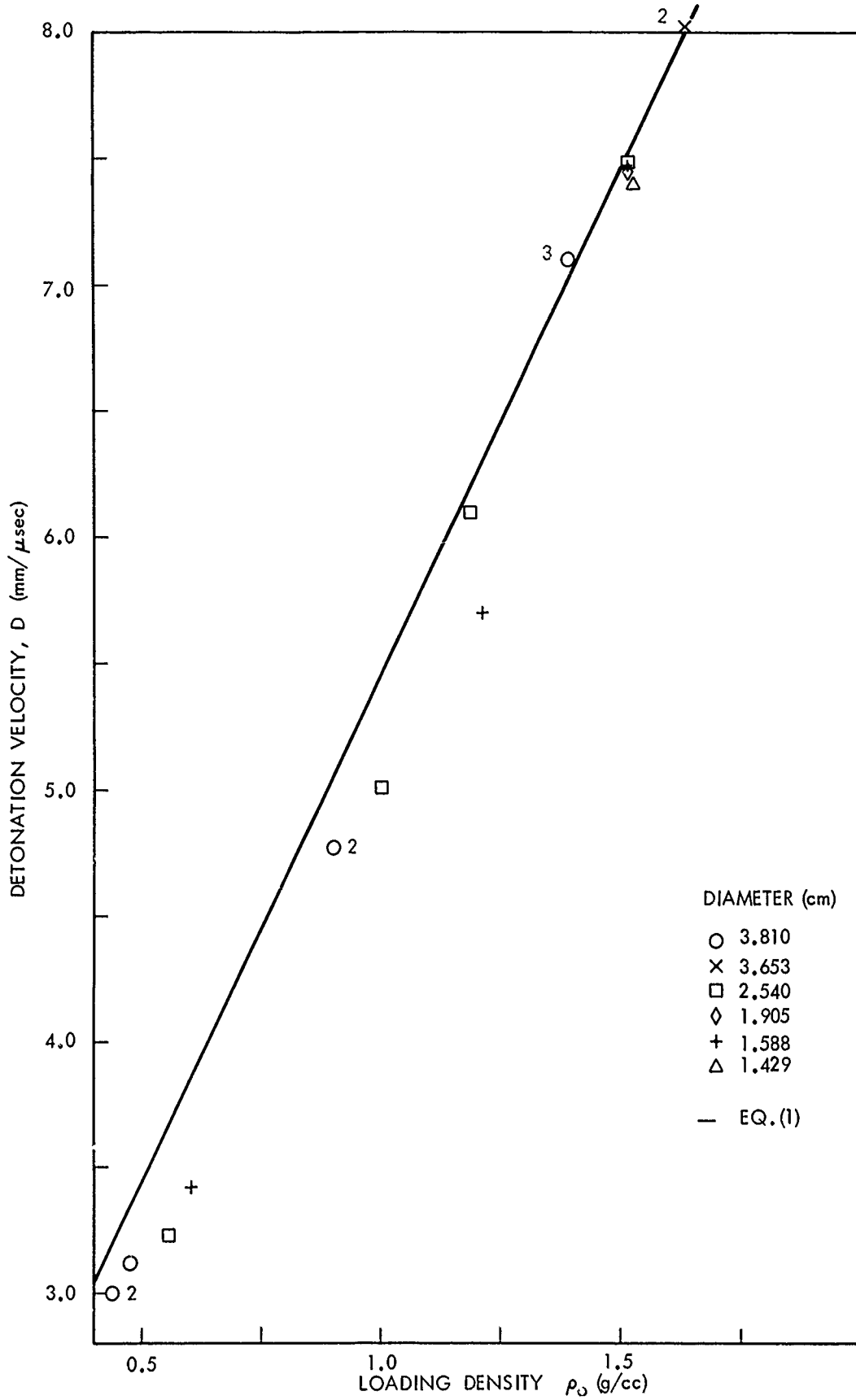


FIG. 4 COMPARISON OF DETONATION BEHAVIOR OF NQ (LBD) WITH IDEAL CURVE

TABLE 5
 DETONABILITY LIMIT DATA FOR NQ (LBD) X547

ρ_0 (g/cc)	d_c (cm)	
	+	-
1.00	2.54	-
1.21	1.59	1.43
1.52	1.43	1.27

d (cm)	ρ_c (g/cc)	
	+	-
1.43	1.52	1.21

NQ (HBD)

Table 6 contains the constant velocity measurements for high bulk density NQ, X530, as a function of diameter and loading density. The behaviors of this coarse particle sized explosive under shock are detonation, pseudo-detonation, and failure.

a. Detonation. The detonation pattern of NQ (HBD) is illustrated in Fig. 8. Like Group 1 explosives, the originating point for the D vs ρ_0 curves of different diameters is on the ideal curve at the high density end. (Points above the ideal curve exceed D_1 only by the order of magnitude of experimental error and also of that of the correction, which has not been made, for a non-planar initiating shock front.) From the originating point the curves fan out with slopes that increase as the diameter decreases.

The failure at highest densities (dead pressing) is not generally observed with the commoner Group 1 materials. It has been described and discussed in a previous section. The failure at the low density end of the 3.81 cm diameter curve was the usual one to be expected with approach to critical density. Failure at the low density end of the 5.08 cm curve is not as clear-cut. Of the four charges at $\rho_0 \sim 1.3$ g/cc, two were prepared in the isostatic press; their data

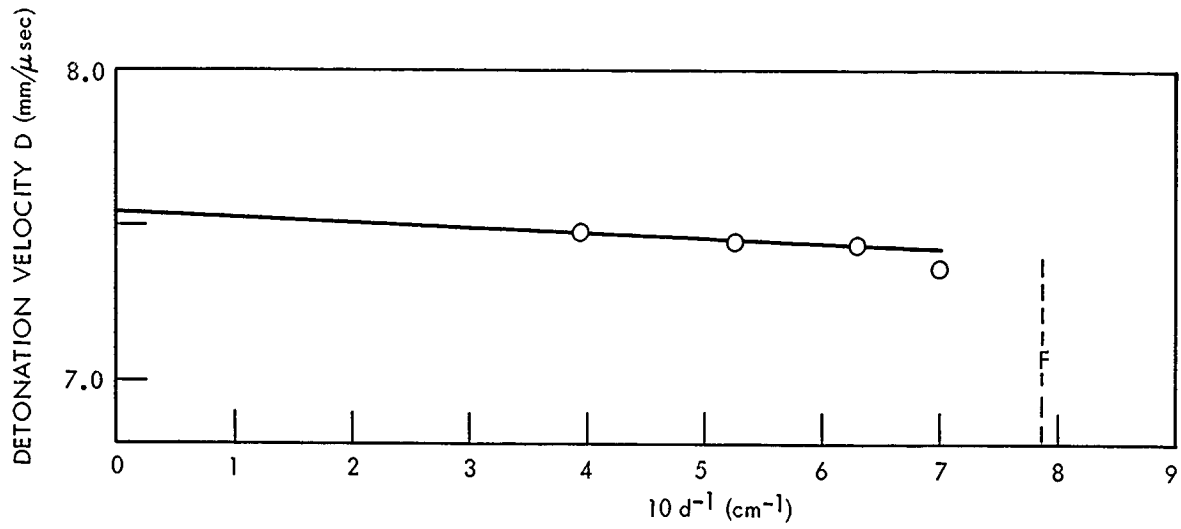


FIG. 5 DIAMETER EFFECT AT $\rho_0 = 1.514$ g/cc FOR NQ (LBD)

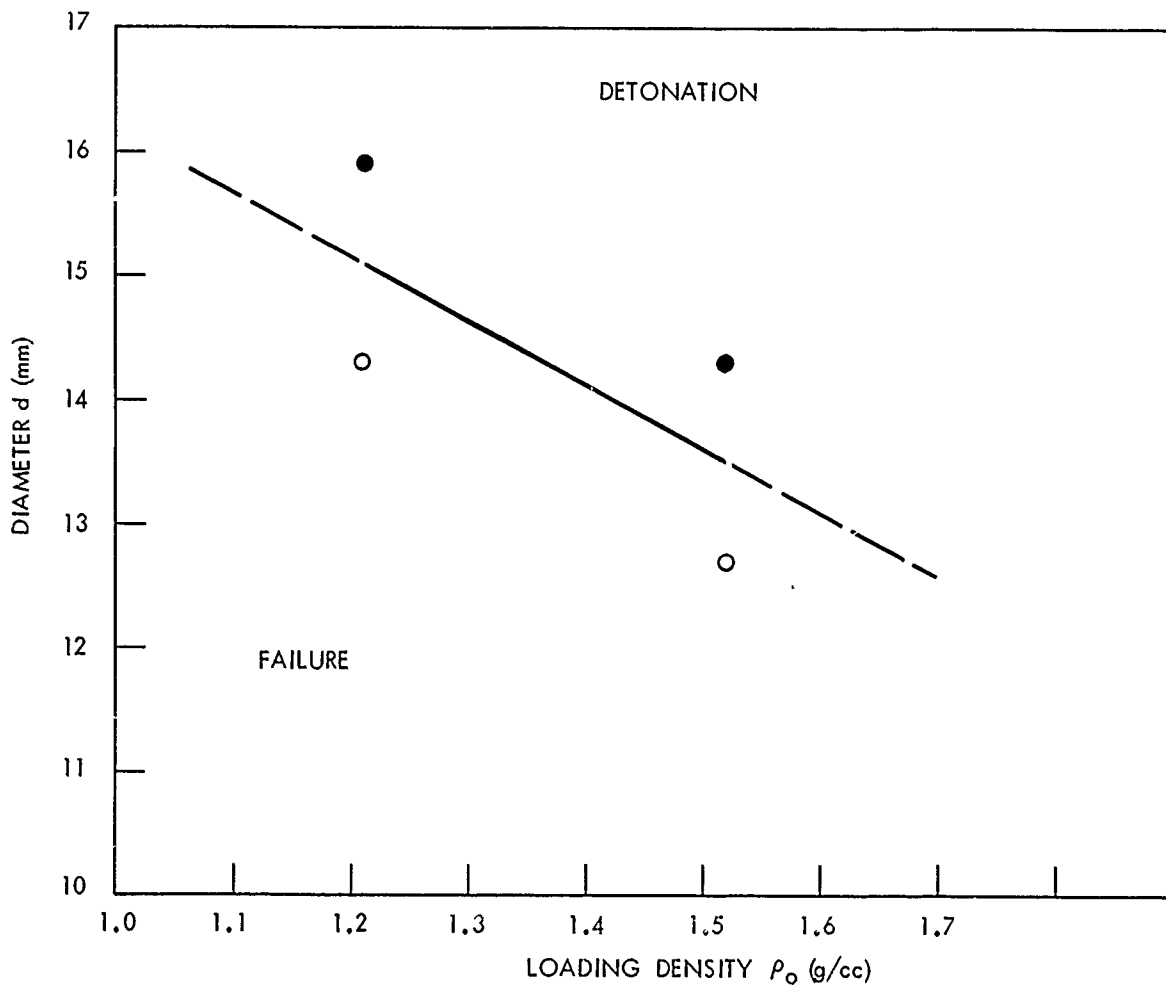


FIG. 6 SECTION OF LIMIT CURVE FOR NQ (LBD) X547

appear at the lower end of the linear portion of the 5.08 cm diameter D vs ρ_0 curve. The other two, prepared in the hydraulic press, had lower velocities. However, the apparent difference might arise from differences caused by different effective densities resulting from the two different methods of compaction. The points at 1.20 and 1.25 g/cc are also measurements made on charges prepared in the hydraulic press. Although the record for the lower density charge shows the familiar curvature obtained in failures, the record for the charge of 1.25 g/cc showed constant velocity. In other words, the D vs ρ_0 curve for $d = 5.08$ cm instead of terminating abruptly at the end of its linear portion, appears to fall rapidly as it approaches ρ_c . This may occur at other diameters and remain undetected because the experimental charge densities chosen were spaced too far apart.

The diameter effect on D , although somewhat more obvious for the NQ (HBD) data than for the NQ (LBD) data of Fig. 4, is still very small. When the D vs d data of Table 6 at $\rho_0 = 1.615 - 1.626$ g/cc are corrected to $\rho_0 = 1.620$ g/cc, they show no detectable trend (see Table 7). This is, in part, because the diameter effect at high ρ_0 is no larger than experimental error; in part, because NQ (HBD) is a coarse material with which it is hard to duplicate charges. The mean value is 7.98 mm/ μ sec ($\sigma = 0.030$) and compares well to the two point average for NQ (LBD), at $d = 3.65$ cm and corrected to $\rho_0 = 1.620$ g/cc, of 7.99 mm/ μ sec. Both are slightly higher than the ideal value of 7.94 mm/ μ sec from Eq(1).

TABLE 7
LACK OF DIAMETER EFFECT ON D OF NQ (HBD)

<u>d(cm)</u>	<u>D(mm/μsec)*</u>
5.08	7.963
4.44	7.994
4.13	7.969
3.97	7.933
3.81	8.026
3.81	<u>7.997</u>
* $\rho_0 = 1.629$ /cc	Average 7.980 ($\sigma = 0.030$)

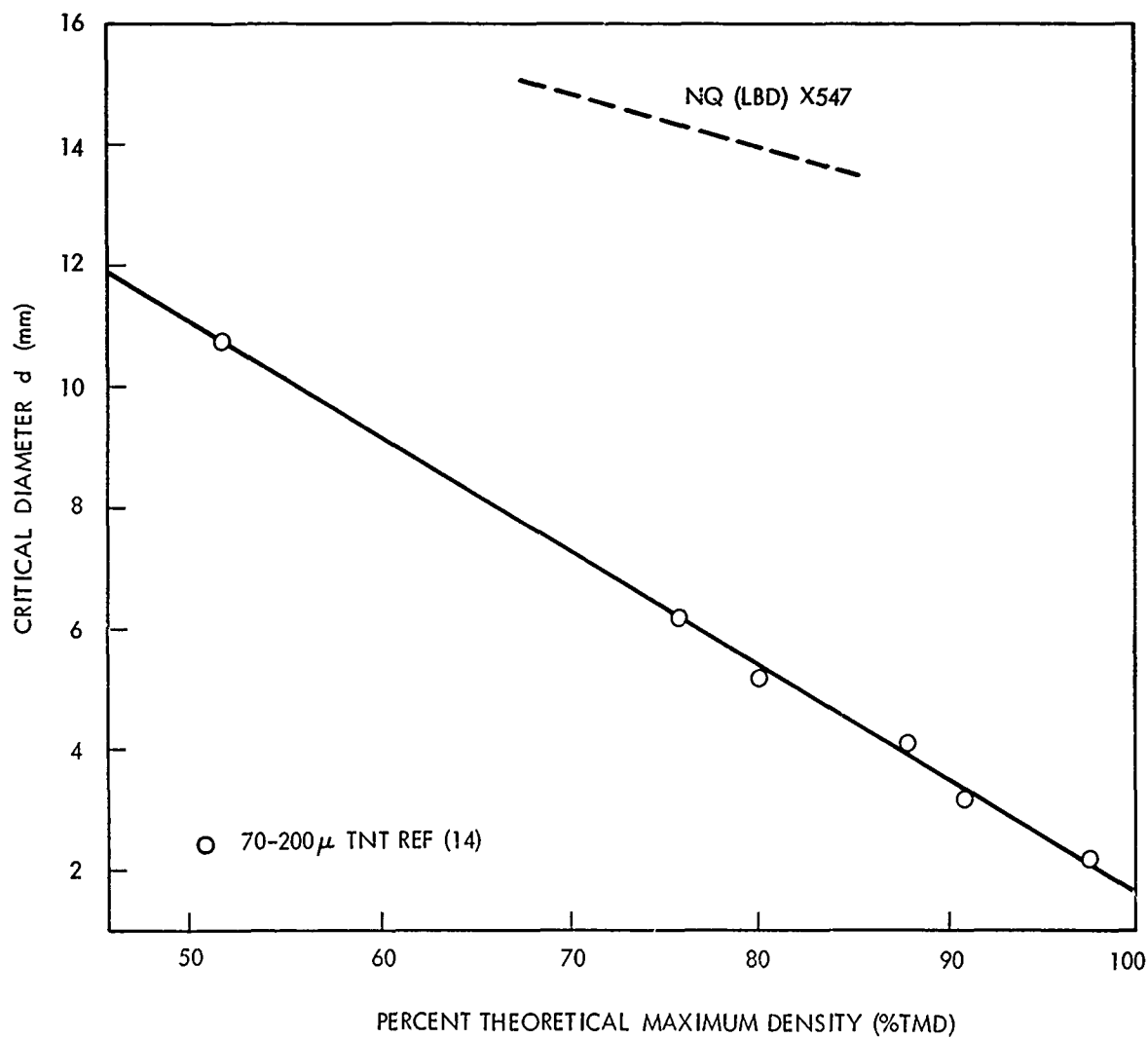


FIG. 7 COMPARISON OF LIMIT CURVES FOR COARSE TNT AND NQ(LBD)

TABLE 6
CONSTANT VELOCITY DATA FOR NQ (HBD) X530

ρ_0 (g/cc)	Front Velocity* mm/ μ sec	Shot No.	ρ_0 (g/cc)	Front Velocity* mm/ μ sec	Shot No.	Fade-out distance, diameters
$d = 7.62$ cm; $(L/d) = 2.7$			$d = 4.128$ cm; $(L/d) = 4.9$			
1.001h	4.833	326	1.6201	7.969	303	
1.198H	5.681	327	$d = 3.969$ cm; $(L/d) = 5.1$			
1.4221	7.075	328	1.6221	7.941	309	
$d = 5.08$ cm; $(L/d) = 4.0$			$d = 3.81$ cm; $(L/d) = 5.2$			
0.718h	3.211	276	0.735h	2.942	268*	
0.851h	3.554	291	0.735h	2.874	270*	
1.001h	3.735	277*	0.851h	3.188	288	
1.001h	3.769	292*	1.001h	3.210	269 ^a	
1.051h	3.827	306	1.009h	3.208	266 ^a	
1.101h	3.754	316 ^b	1.101h	3.109	289	
1.102h	3.784	293 ^b	1.202H	F(2.15)	290	
1.200H	F(4.88)	305	1.295H	F(3.44)	325	
1.251H	5.579	310	1.3031	F(3.34)	267	
1.292H	6.279	330	1.3071	F(3.28)	265	
1.299H	6.125	318	1.3611	F(4.11)	329	
1.2991	6.518	279	1.4011	6.723	331	
1.3041	6.502	317	1.4141	6.841	314	
1.4081	7.062	282	1.6221	8.034	311	
1.4641	7.226	304	1.6201	7.997	312	
1.5121	7.493	281	1.6681	F(5.56)	271	1.9
1.5311	7.640	273	1.6651	F(2.88)	315	1.9
1.6261	7.987	280				
$d = 4.445$ cm; $(L/d) = 4.6$						
1.6151	7.974	294				

TABLE 6 (Con't)

ρ_0 (g/cc)	Velocity* mm/ μ sec	Shot No.	Fade-out distance, diameters
$d = 3.651$ cm; $(L/d) = 5.6$			
1.6171	F	313	2.5
$d = 2.54$ cm; $(L/d) = 8.0$			
0.72h	2.345	260*	
0.72h	2.352	264*	
0.851h	2.568	308	
1.001h	2.580	259*	
1.001h	2.500	263*	
1.101h	F(2.25)	307	6.6
1.2941	F	251	2.2
1.2941	F(<2.25)	254	2.3
1.6751	F	249	2.0
1.6751	F	250	2.2
$d = 1.5875$ cm; $(L/d) = 12.8$			
0.704h	1.781	255*	
0.709h	1.851	252*	
0.715h	1.854	248**	
0.850h	1.897	253*	
0.850h	1.963	256*	
0.850h	1.981	261*	
0.850h	1.983	262*	
1.002h	F(1.96)	257	4.6
1.002h	F(2.09)	258	4.6
1.009h	F	247	<5.6
1.2831	F	244	<2.4
1.2831	F	245	2.0
1.6781	F	243	<2.2
1.6781	F**	246	<2.8

Averaged values of ρ_0 and velocity, respectively:

- a. 1.001, 3.752(2); b. 1.102, 3.769(2);
- c. 0.735, 2.908(2); d. 1.004, 3.209(2);
- e. 0.72, 2.348(2); f. 1.001, 2.540(2);
- g. 0.709, 1.829(3); k. 0.850, 1.956(4).

* Number in parentheses after F is velocity of falling shock.

**Stronger booster. Other symbols as in Table 3.

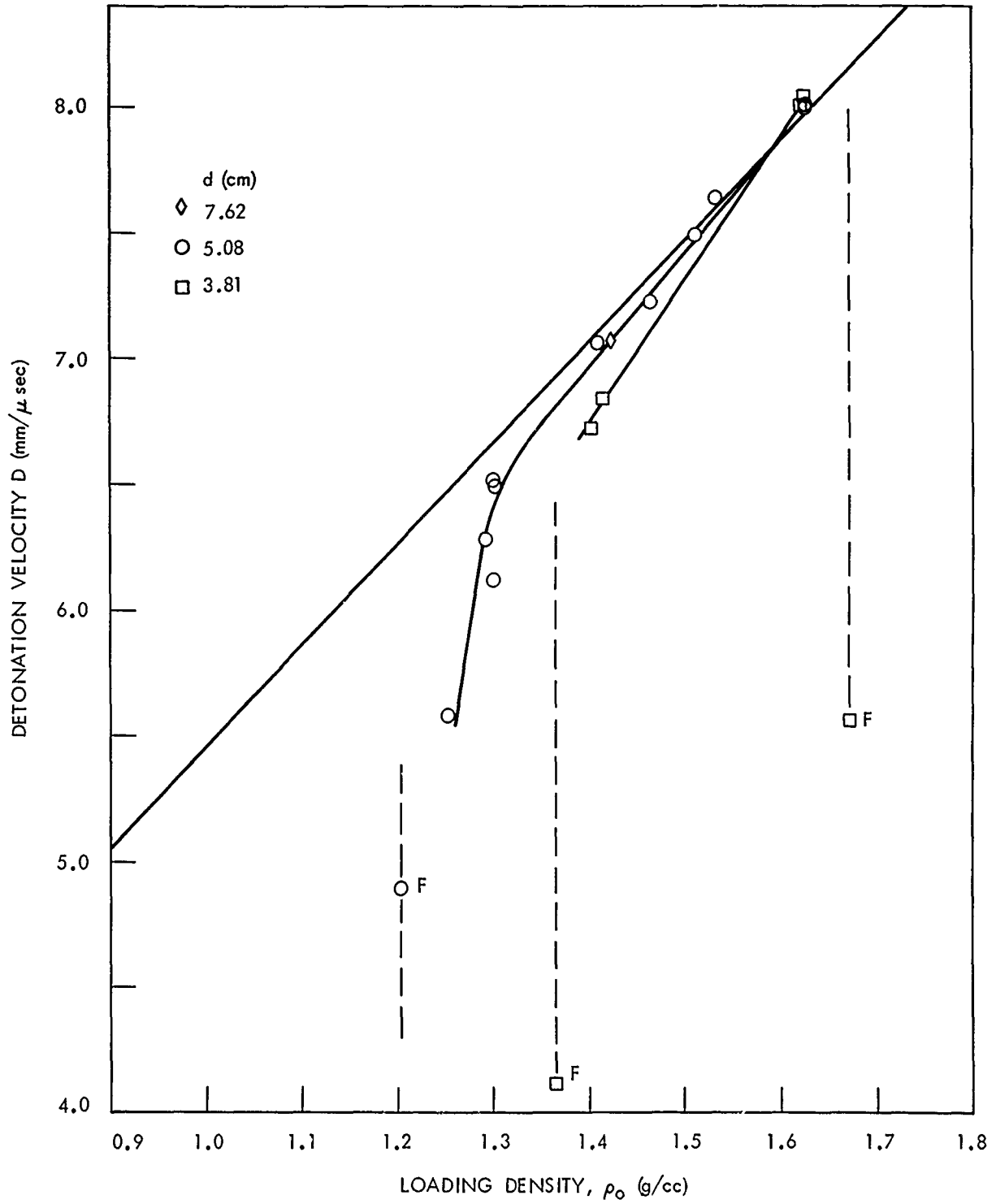


FIG. 8 DETONATION BEHAVIOR OF NQ (HBD), X530

The limit data for detonation of NQ X530 are collected in Table 8 and plotted in Fig. 9 which also shows the failure curve for NQ (LBD) X547. It is evident that NQ (HBD), like NQ (LBD), shows the Group 1 trend of increasing d_c with decreasing ρ_c . In view of the difference in particle size and shape, it is not surprising that the NQ (LBD) curve lies well below that for NQ (HBD) nor that the "dead-pressing" phenomenon, if it exists in NQ (LBD), occurs at a higher density than in NQ (HBD). The highest density we achieved for the LBD material was 1.627 g/cc at $d = 3.65$ cm; it detonated at these conditions whereas the NQ (HBD) failed at 1.617 g/cc.

TABLE 8
CRITICAL DATA FOR DETONATION OF NQ (HBD) X530

ρ_0 (g/cc)		d (cm)	
+	-	+	-
1.63	1.67		3.81
	1.62	3.81	3.65
1.40	1.36		3.81
1.25	1.20		5.08
	1.00	7.62	-

b. Pseudo Detonation. In the lower density region, shocked NQ (HBD) exhibits a diameter and density dependent constant front velocity well below that of the ideal curve. The behavior observed is illustrated in Fig. 10 which covers the region of what we shall call pseudo detonation or LVD (for the term "low velocity detonation" which frequently appears in the literature).

The phenomenon of LVD is well established for liquid explosives, particularly for nitroglycerin which has been extensively studied.

For solid explosives, many reported instances of LVD are obviously transient states encountered in the course of buildup to detonation. There are, however, a few instances of sub-detonation but supersonic constant velocities persisting for great distances.

Patterson¹⁵ first noted that a 1.5 in. diameter cartridge of blasting gelatin (NG and NC) exhibited a constant velocity of about 2.4 mm/ μ sec without any sign of fading over a length of at least 17 ft. He also found that at cartridge diameters of 7/8 to 2 in., either detonation ($D \sim 8$ mm/ μ sec) or LVD could be initiated according to the power of the booster used; that above $d = 2$ in. only detonation was stable, i.e., a reaction front initially moving at lower velocities would accelerate to D if the cartridge were long enough. Other workers noted that the blasting gelatin must have some aeration to exhibit LVD and that frequently some unburned explosive can be recovered after LVD has traversed the cartridge.

An earlier reference and one more relevant to the present work is that of Jones and Mitchell.¹⁶ They too used detonators of different power on coarse granular charges of TNT. They report, "by using a sufficiently narrow cartridge, or, alternatively, a sufficiently coarse grist of explosive, the low-order detonation can be made to travel throughout the length of the cartridge (at least a meter) at a rate which is both uniform and repeatable.----- On the other hand, if a sufficiently powerful initiator is used, the same cartridge propagates detonation at a greatly enhanced speed, the rate of detonation being again uniform and repeatable." They too comment on the presence of undecomposed explosive residue after LVD.

Recently, Parfenov and Apin¹⁷, have studied coarse granular low density charges of tetryl, TNT, and RDX. For each material, ρ_0 was fixed (~ 1.0 g/cc) and the diameter varied in the range of 5 to 40 mm. The ratio l/d was kept ≥ 10 . The particle sizes used were 1000-1600 μ , 630-1000 μ , and 400-630 μ for tetryl; 400-630 μ for TNT, and 1000-1600 μ for RDX. As in the previous two references, initiators of high and low power were used. In all three H.E., regions of detonation and of LVD were reported. For TNT and RDX, these regions showed

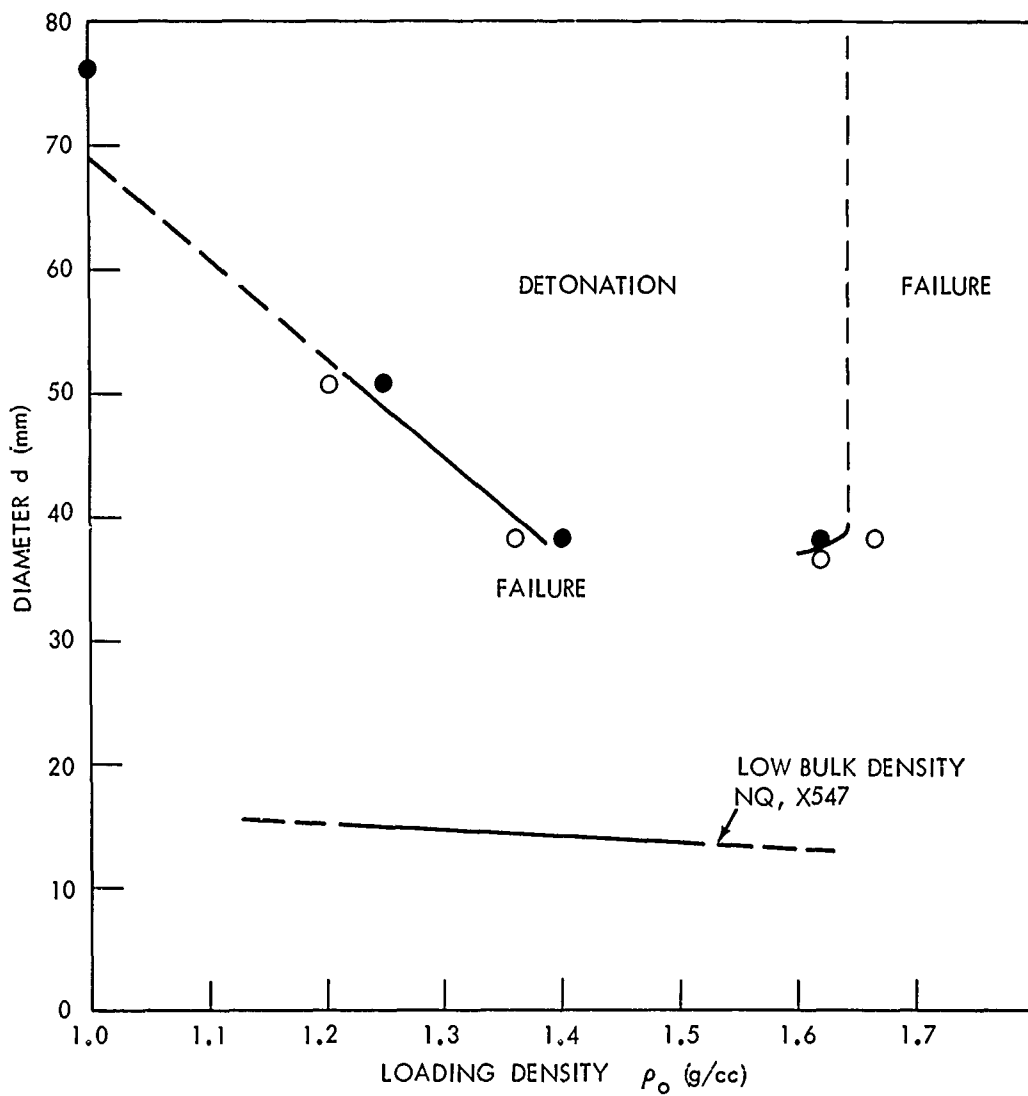


FIG. 9 SECTIONS OF LIMIT CURVE FOR DETONATION OF NQ (HBD) X530

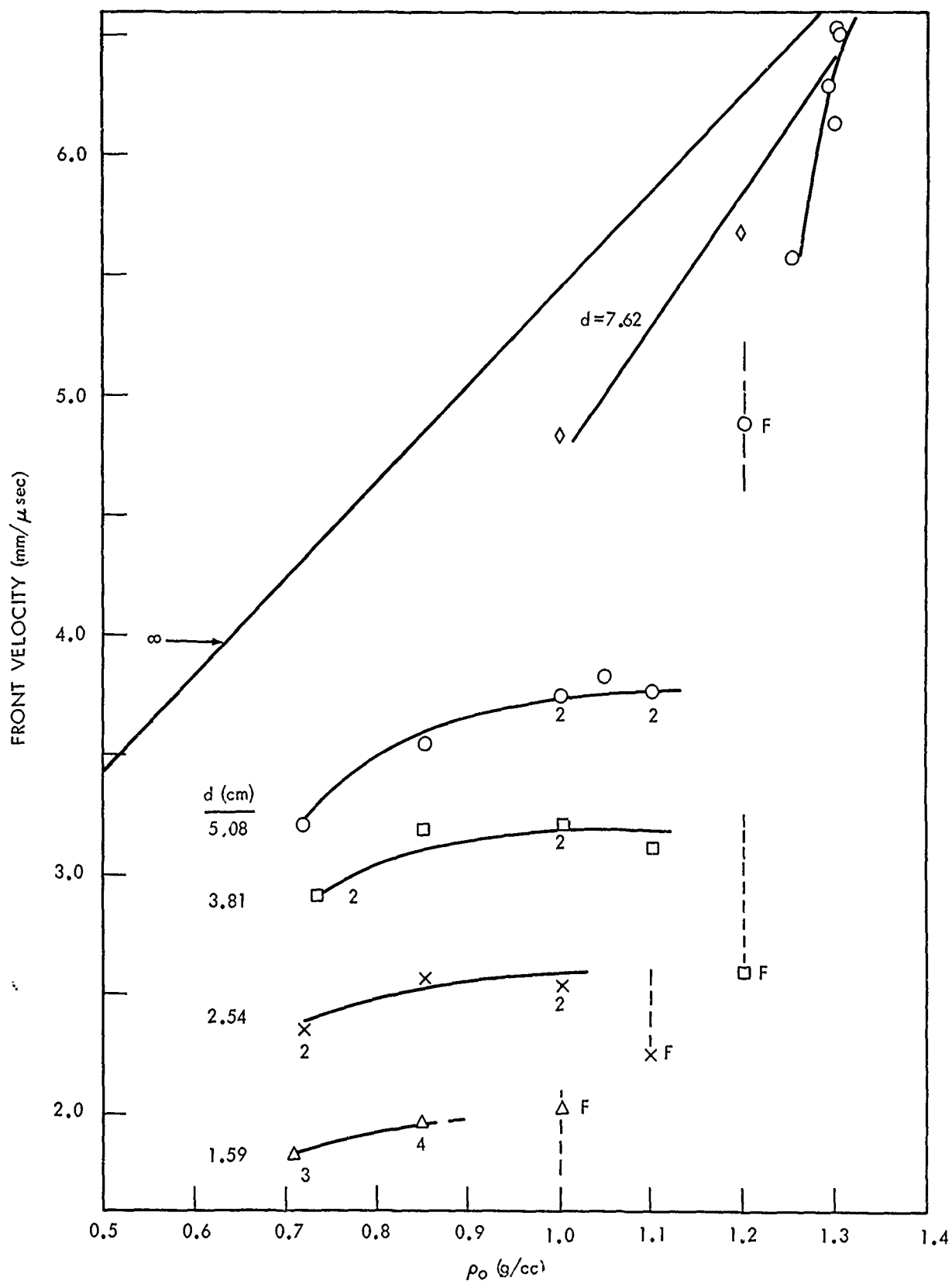


FIG. 10 PSEUDO DETONATION (LVD) BEHAVIOR OF NQ (HBD), X530

overlap*, but for tetryl they were sharply divided at $d = d_c$ for detonation. Consequently the division was also detectable when only the high powered initiator was used. Gurton¹⁸, on the other hand, reports an apparent overlap for another coarse tetryl (pour density of 0.9 g/cc, particle size not reported). At $d = 1.11$ cm (7/16 in.), Gurton reported 1.5 and 4.6 mm/ μ sec obtained respectively with weak and strong initiation. The latter figure is quite close to the ideal velocity for this density, and the former is in the range of LVD measurements of Ref. 17. It is also possible that 11.1 mm was about the critical diameter (it is near the d_c values of Ref. 17); if so, the two sets of data^{17,18} are completely consistent.

It is our opinion that the pattern of Fig. 10 is caused by a similar LVD phenomenon which is detected with our powerful initiator only at diameters below the critical value for detonation. It is possible, of course, that a weaker initiator might extend the LVD curves to higher ρ_0 , but the shock velocities in the failures (indicated as F in Fig. 10) are generally lower than the constant value of the LVD at $d = 1.59$ - 3.81 cm. For that reason a weaker initiator would not be expected to extend the LVD curves.

In detonation of a pure H.E., the diameter effect on D is found experimentally to be

$$D = \alpha + \beta/d \quad \alpha, \beta, \rho_0 \text{ constant} \quad (2)$$

and $d \gg d_c$

If we let U_{LV} = the constant but pseudo detonation velocities of Fig. 10

$$U_{LV} - 1.42 = (d^n - 1) (3.29 - 1.08 \rho_0) \quad (3)$$

where U, d, and ρ_0 are in mm/ μ sec, cm, and g/cc, respectively, and

$$n \approx 0.129 + 0.316 \rho_0 \approx 0.445 \rho_0^{0.7}$$

The ranges for Eq(3) are 0.75 to 1.0 g/cc and 1.59 to 5.08 cm in ρ_0 and d respectively.

*The overlap was in the diameter range of the velocity vs d curve, i.e., for some d values either detonation or LVD occurred according to the kind of initiation. It is interesting that the coarse TNT exhibited $d_c \approx 24$ mm at $\rho_0 = 0.95$ g/cc (about twice the d_c for the finer material of Fig. 7) and that LVD was observed in the range 23-30 mm.

It is quite evident that the diameter dependence of U_{LV} Eq(3) is very different from that of D Eq(2). Similarly the dependence on ρ_0 differs because, experimentally, Group 1 explosives show

$$D = A' + B'\rho_0, \quad A', B', \text{ and } d \text{ constant}$$

or $d > d_c$

$D(d, \rho_0) = A + B\rho_0 - \beta(\rho_0)/d$ where A, B are constants for the infinite diameter curve and $\beta(\rho_0)$ seems to be a linear function of ρ_0 .

For these reasons as well as the termination of the detonation curves shown in Figs. 8 and 10, the phenomena described by Eq(3) are considered pseudo-detonation or LVD. We do not mean to suggest by this term that the reaction involved in LVD is necessarily very weak. Even at its lowest velocities (~ 2 mm/ μ sec at $d \sim 1.6$ cm and $\rho_0 \sim 0.8$ g/cc) it was able to initiate an explosive witness placed at the end of the charge. At higher velocities it appears well able to damage steel plates.

Fig. 10 shows a previously unreported area of failure (1.20 to 1.36 g/cc in extent) separating the region of LVD from the region of detonation for the curves obtained with charges of $d = 3.81$ cm. But because previous investigators^{16, 17, 18} restricted themselves to a constant charge density (and a low one) for granular charges, they could not observe such a density dependent failure phenomenon. In view of our own difficulty in sharply dividing pseudo-detonation from detonation behavior in the moderately sized charges ($d = 5.08$ cm), it is fortuitous that we happened to choose the charge size of $d = 3.81$ cm at which such a failure area seems clearly evident. The smaller charges ($d = 1.59$ to 2.54 cm) exhibited only LVD and were evidently subcritical for detonation over the entire density range tested.

The trends of Fig. 10 indicate that as the charge diameter is increased, the LVD region approaches the detonation region. At sufficiently large diameter, therefore, only detonation should be observed. This trend is perhaps more evident when the data at fixed charged density are plotted as front velocity vs charge diameter.

This has been done in Fig. 11 for NQ, X530 at $\rho_0 = 0.85$ g/cc where it is compared with the Russian curve¹⁷ for coarse tetryl at $\rho_0 = 0.90$ g/cc. Parfenov and Apin¹⁷ found that the tetryl exhibited LVD at $d \leq d_c$, detonation at $d \geq d_c$. Because the critical diameter for detonation of NQ X530 at $\rho_0 = 0.85$ g/cc is much greater than that of the tetryl (See Fig. 9), the entire range of diameters in Fig. 11 is subcritical for NQ. At some large diameter, NQ, like the tetryl, would probably exhibit a discontinuous charge from LVD to detonation.

As Fig. 10 also shows, there exists a failure or limit curve for the LVD behavior. The critical data, collected in Table 9 and plotted in Fig. 12, emphasize the interesting fact that the limit curve for LVD (Fig. 12) is exactly opposite in trend to the limit curve for detonation (Fig. 9). Moreover the limit behavior for LVD (increasing diameter with increasing density) parallels the Group 2 limit behavior for detonation. It seems most likely, therefore, that it was an LVD reaction which was responsible for an increasing output with decreasing %TMD when NQ (HBD) was tested in the small scale gap test.¹ It also seems highly probable from the dents produced that reactions in at least a part of the LVD region will be quite powerful enough to exhibit a positive result on the regular large scale gap test.

TABLE 9
LIMIT DATA FOR PSEUDO DETONATION OF NQ (HBD)

Diameter <u>d (cm)</u>	Density ρ_0 (g/cc)	
	<u>+</u>	<u>-</u>
1.59	0.85	1.00
2.54	1.00	1.10
3.81	1.10	1.20
5.08	1.10	1.20

The usual qualitative explanation for an LVD reaction is that it is supported by the explosive decomposition of only a fraction of the H.E. present. If as Ref. 16 suggests, LVD can be observed in solids

only when they are coarse granular materials, it is possible that its propagation depends on a hot gas flow through a granular bed exhibiting a particular porosity. But it is difficult to consider such a mechanism applicable to blasting gelatin even when it contains some aerated areas. The concepts of partial reaction and surface reaction do seem applicable in both cases.

The mechanism of pseudo-detonation which seems most acceptable, however, is that suggested in 1962 by Bowden.¹⁹ It consists of an ignition wave coupled to a shock wave, e.g., a shock wave travelling through crystal of explosive, which contains a number of imperfections, ignites the explosive at the site of each imperfection.¹⁹ The ignition wave travels at the shockwave velocity although the deflagration, that continues at each ignition site after the shockwave has passed, progresses at a much slower, subsonic rate.

Imperfections in a single crystal serve as heterogeneous areas where energy concentration and hence ignition can occur. In granular explosives, there is probably a range in grain sizes and shapes which favor hot spot formation on grain surfaces when the grain bed is shocked. (Local concentration of energy could occur by reflection and reinforcement of the initial shock and by spalling or jetting of the shocked grains.) If the physical characteristics of the granular bed are such as to produce numerous, well distributed sites of ignition, such shock-produced hot spots can result in the continuous smear camera record of a pseudo-detonation. The grain size favoring pseudo-detonation will depend on the material. Thus, for the relatively sensitive tetryl ($\rho_0 = 0.90$ g/cc), it is reported at a grain size of 400-1600 μ and $d < d_c = 12$ mm.¹⁷ But for the less sensitive NQ, X530 ($\rho_0 = 0.85$ g/cc) it is found at a grain size of up to 200 μ (average about 100 μ) and $d = 16 - 50$ mm. It has not been observed at all in the low bulk density NQ* which has thin needle crystals of 50 - 100 μ length.

*Attempts made to initiate LVD in NQ (LBD) with weak initiators were unsuccessful. Gurton¹⁸ refers to LVD of a NQ (LED) at $\rho_0 = 0.5$ g/cc and $d = 1.1$ to 1.9 cm, but he measured the same velocities for both weak and strong initiation. Since the velocities were also high (80 - 90% ideal for $\rho_0 = 0.5$ g/cc), it is probable that the phenomenon he observed was detonation.

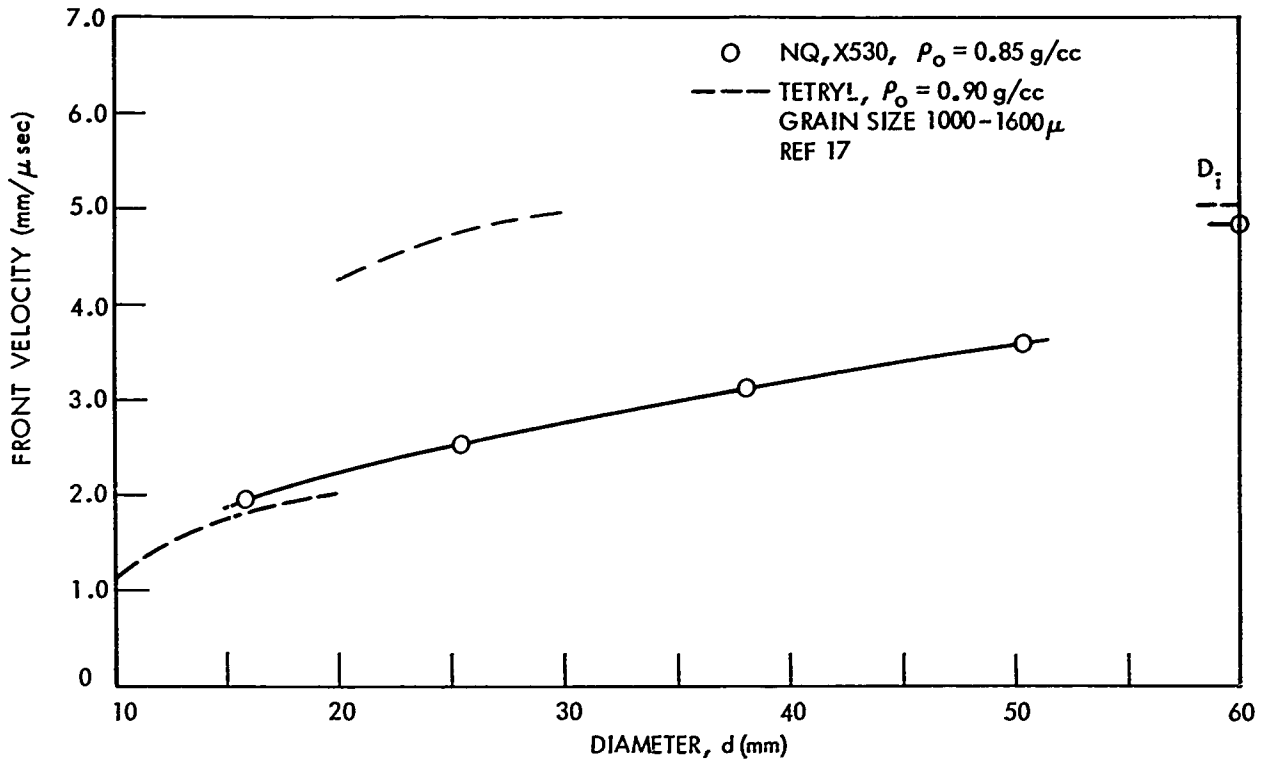


FIG. 11 COMPARISON OF DIAMETER DEPENDENCE OF LVD IN TETRYL AND NQ (X530)

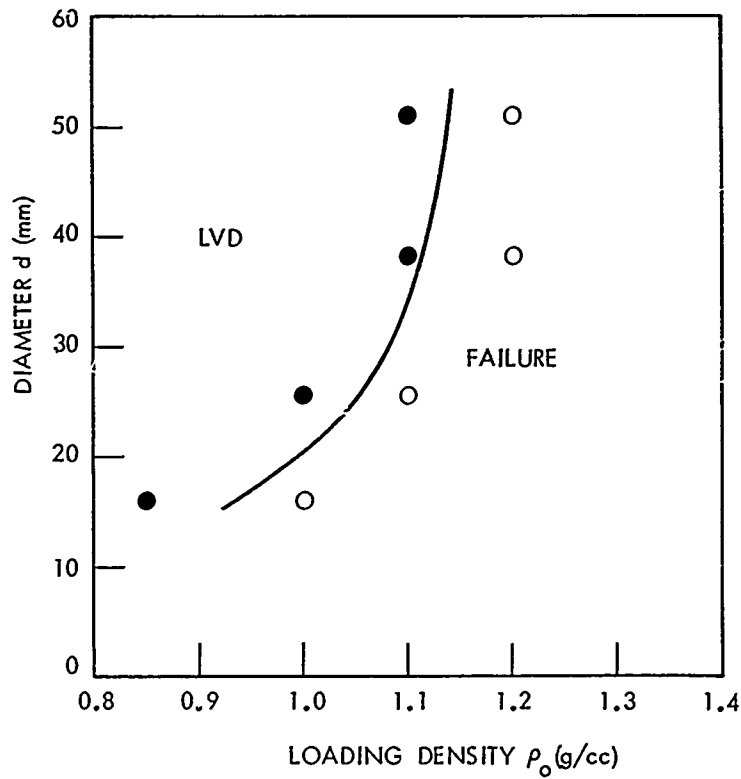


FIG. 12 LIMIT CURVE FOR PSEUDO-DETONATION OF NQ (HBD), X530

The instantaneous reaction and energy release at the hot spots, although amounting to only a small fraction of the total chemical energy of the explosive, is sufficient to contribute to the shock wave energy to the extent of producing an essentially constant velocity front. Moreover, in every case the energy release resulted in a pressure at the surface of the pentolite witness sufficiently high to initiate almost immediate detonation of the pentolite (See Fig. 2). Initiation of pentolite very near the shocked surface, i.e., a run-length of a few mm, requires shock pressures of about 40 kbar although the minimum initiating pressure (run length of up to two diameters from the shocked surface) is perhaps 10 kbar. The pressure of about 40 kbar, indicated by the behavior of the pentolite witness, is of the order of magnitude required to punch the steel witness plate in the standard gap test of shock sensitivity. It is therefore to be expected that some of the pseudo-detonation reactions will exhibit positive results in the gap test.

c. Effect of Particle Size. We have assumed that the major differences in behavior between NQ (LBD) and NQ (HBD) in the lower ρ_0 range arises from the difference in particle size. [In the higher ρ_0 range where both materials are detonable, they differ markedly in detonability (Fig. 9) but not in detonation velocity after initiation.] But because of the very different particle shapes in the two forms of NQ, it seemed desirable to compare a sample of NQ (HBD) with the same material after it had been ground to a smaller particle size.

For this purpose, NQ (HBD) X589 was obtained; its screen analysis was similar to that of X530 (See Appendix A). A sample of X589 was then ground until it contained a large number (at least 50%) of fines; the ground material was designated X588. Table 10 contains the detonation velocity data obtained for comparison of these two materials.

X589 appears coarser than X530; it exhibits failure at $\rho_0 = 1.0$ g/cc whereas X530 shows LVD here. Grinding X589 makes it effectively

much finer than X530. For example, 5.08 cm charges of X588 exhibit velocities equal those of the 7.62 cm charges of X530. Moreover, at 5.08 cm diameter, NQ X588 is detonating at D of 0.88, 0.93, and 0.99 D_1 , respectively, for ρ_0 values of 1.0, 1.2, and 1.35 g/cc. Hence, decreasing the particle size by grinding has eliminated the LVD region of Fig. 10 at this diameter. Increasing the diameter can also eliminate the LVD region. For any given material, the ratio of its particle size to its charge diameter and its shock sensitivity probably determine whether LVD appears.

Shock Sensitivity

The regular gap test²⁰ has been used to investigate the shock-to-detonation sensitivity of various lots of NQ in the past. These earlier test results are collected in Table 11 and plotted in Fig. 13. Three production lots of NQ (HBD) from NOS fell on the same P_g vs ρ_0 curve despite average particle size variation of 38-100 μ . Moreover, all three lots confirmed the existence of the unusual hump in the curve between 75 and 85% TMD. Heretofore we have had no suggested explanations for this peculiarity. In view of the present work we can surmise that it might be caused when the induced reaction is an LVD rather than detonation.

Aside from the small hump on the lower curve, the trends of Fig. 13 seem normal. NQ (HBD) approaches its "dead-pressed" density in the gap test configuration at about 92% TMD (1.64 g/cc); this compares well to slightly above 1.626 g/cc, the value found in the work on unconfined charges of $d = 5.08$ cm. At this high density, the diameter effect is negligibly small; hence the unconfined and confined charges should exhibit the same critical density for detonation. The sensitivity curve for NQ (LBD) lies slightly above that for the high density material and approaches the lower curve at the greatest compaction. It, however, shows no hump and is very like P_g vs TMD curves of other H.E. (See, for example, Ref 1) The difference, NQ (LBD) less shock sensitive than NQ (HBD), is that expected when the chief difference between lots is a difference in particle size. Generally the finer material, if it differs at all from the coarser, shows lower shock sensitivity in a granular charge¹.

NOLTR 67-169

TABLE 10

DATA FROM NQ'S X530, X588, AND X589

<u>NQ</u>	<u>ρ_0 g/cc</u>	<u>Front Velocity mm/μsec</u>	<u>Shot No.</u>
<u>$d = 5.08$ cm; $(l/d) = 4.0$</u>			
X589	1.001h	F(3.54) ^a	397
	1.201H	F(4.14)	396
	1.4271	7.067	395
	1.4331	7.169	399
X588 ^b	1.001h	4.803	411
	1.202H	5.805	410
	1.3511	6.797	409

Effect of Particle Size

<u>NQ</u>	<u>d</u>	<u>Front Velocity</u>			<u>Relative Particle Size</u>
		<u>ρ_0: 1.00</u>	<u>1.20</u>	<u>1.43</u>	
X589	5.08	F	F	7.12	Coarse
X530	5.08	3.76	F	7.10 ^c	Less coarse
X588	5.08	4.80	5.80	--	Least coarse

<u>NQ</u>	<u>d</u>	<u>Front Velocity</u>			
		<u>ρ_0: 1.00</u>	<u>1.20</u>	<u>1.35</u>	
X588	5.08	4.80	5.80	6.80	Fine
X530	7.62	4.83	5.68	6.74 ^c	Coarse

^a F means failed. Number in parentheses is velocity of failing shock.

^b X589 ground. See Appendix A

^c Read from Fig. 8

The hump in the NQ (HBD) curve of Fig. 13 is at about 79% TMD or 1.41 g/cc. This is about the critical density for 3.81 cm diameter unconfined charges of NQ, X530 (See Figs. 8 and 9). The explosive core diameter in the gap test is 3.65 cm, but since the diameter effect is still small* at 1.41 g/cc, the effective diameter for detonation in the gap test should be close to 3.81 cm. Hence it is very near $\rho_0 \sim 1.41$ g/cc that detonation of this NQ would fail in the gap test. The confinement, by providing local shock enhancement by reflection from the steel walls, might well extend the density range of LVD up to the critical density for detonation. In other words, the containing steel tube which would have little effect on detonability at this density might so enhance the possibility of LVD that the pseudo-detonation can occur at $\rho_0 < \rho_c$. If at charge densities lower than $\rho_0 \sim 1.41$ g/cc LVD does occur, its reaction would be sufficiently powerful to punch the steel witness plate, i.e., to produce a positive result in the gap test.

In accord with the above interpretation, the hump in the P_g vs % TMD curve of Fig. 13 results from a combination of detonability and shock sensitivity behavior near the critical density ρ_c for detonation. At $\rho_0 > \rho_c$, NQ (HBD) detonates and P_g measures its shock sensitivity to detonation; at $\rho_0 < \rho_c$ this NQ exhibits LVD and P_g measures its shock sensitivity to LVD.

If this explanation is correct, other samples of NQ (HBD) which exhibit $\rho_c \sim 1.41$ g/cc should also exhibit a hump in the P_g vs %TMD curve. If such a NQ is ground until it is detonable at lower charge densities, then its shock sensitivity curve should resemble that for other H.E. and be concave upward over the %TMD test range with no hump present.

Table 12 contains the gap test data for X589, a recent production lot of NQ (HBD) and for X588, a sample from the same lot after grinding. Detonation velocity measurements (Table 10) showed that

*For 3.81 cm diameter charges, the D values at 1.5. and 1.41 g/cc are, respectively, 0.98 and 0.96D₁.

TABLE 11
PREVIOUS SHOCK SENSITIVITY TESTS ON NQ

NQ(HBD)	P _o # g/cc	TMD %	50% Point		Comment
			No. Cards	P g kbar	
X311*	1.641	92.1	36	90	Average particle size 51μ X311 screened to 38μ
	1.441	80.9	85	55.5	
X446*	1.641	92.1	32	93	Average particle size 64μ
	1.611	90.6	47	80	
	1.511	85.1	68	64	
	1.401	78.9	~92½	~52	
	1.33H	74.7	128	39	
	1.16h	65.1	196	18	
X510	1.421	79.7	94	54**†	Average particle size 100μ
	1.441	80.7	86	55	
	1.39H	77.9	100	49	
	1.331	74.9	128	39	
NQ(LBD) X547**	1.631	91.4	35	90.0	
	1.511	85.0	60	69.5	
	1.411	78.9	84	56.0	
	1.201	67.4	121	41.5	
	0.901	50.3	194	18.5	
	0.56h	31.2	215½	15.2	

* Reported in NOLTR 65-177
 ** Reported in NOLTR 66-87
 † H hydraulic press, h handpacked, i isostatic press.
 ‡ Pentolite booster.

X589 is apparently a coarser material than X530. It was therefore expected to exhibit a failure to detonate in the gap test and produce a hump in the P_g vs $\%TMD$ curve near the location of the hump in Fig. 13. The data taken in that location (range of 78 - 85% TMD) are plotted in Fig. 14 and show the expected hump. The ground material X588 was shown by detonation velocity measurements to be detonable in this range and should exhibit no hump in its sensitivity curve. As Fig. 14 shows, this is the case and the P_g vs $\%TMD$ curve for X588 in this region is concave upward and approximately parallel to that for NQ (LBD) which is also shown for comparison. The difference between NQ (LBD) and X588 (the latter is more sensitive) is that expected in comparing relatively fine with relatively coarse material. The difference between X588 and X589 is in the opposite direction. An apparent reversal in the usual particle size effect on shock sensitivity could occur if the witness damage is caused by detonation in the one case and LVD in the second.

Two additional aspects of gap testing are worth emphasizing. First, to judge by the velocity pattern of Fig. 10, there is a large range of conditions in which a single shot could not be adequately classified as detonation or LVD. This would be so even for an instrumented gap test (in which detonation velocity or pressure might be measured) because classification requires knowledge of the complete pattern of Fig. 10.

The second point is that the peculiarity in the measured shock sensitivity curve, which is, of course, caused by the test conditions and is not a peculiarity of the true sensitivity, could conceivably occur in any H.E. It is certainly not restricted to NQ although it may be restricted to H.E. which can exhibit LVD. It is not certain that all solid explosives can do this, but it does seem clear that a large grain size and a small charge diameter favor the appearance of LVD.

There is an example in the recent literature^{1,2} in which the gap test results on a coarse (400 μ tetryl) closely paralleled those on NQ (HBD). In a small scale test ($d = 12.7$ mm, charge unconfined),

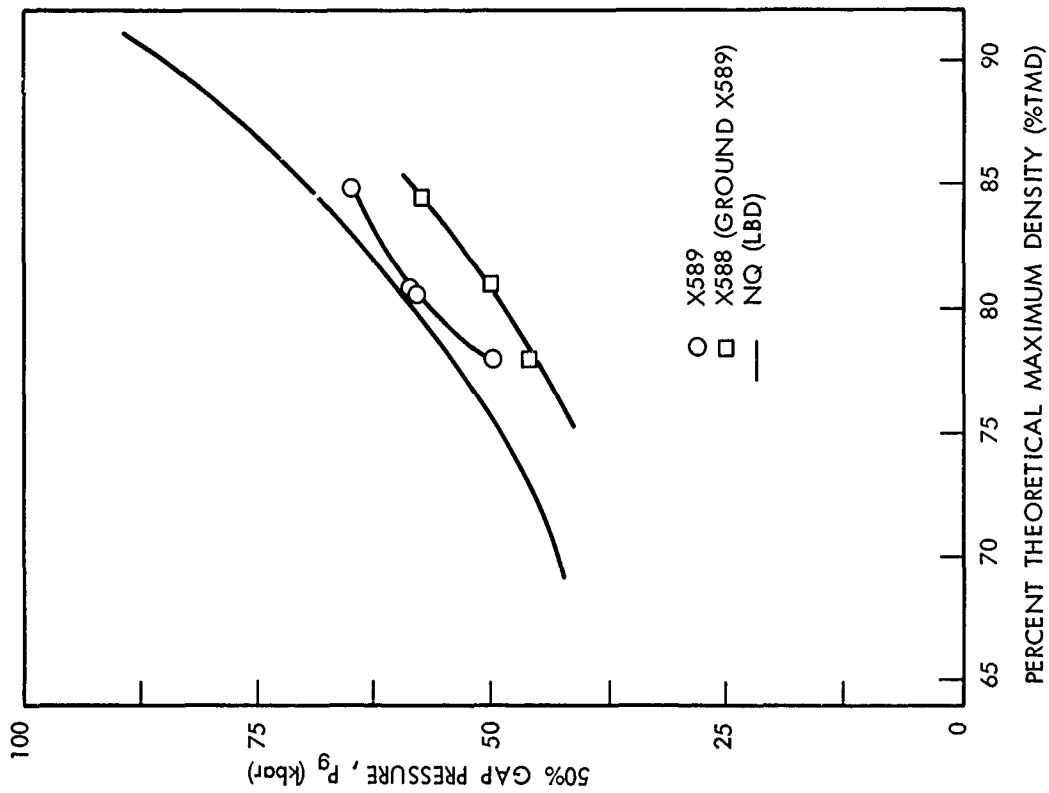


FIG. 14 EFFECT OF GRINDING NQ (HBD) ON ITS SHOCK SENSITIVITY

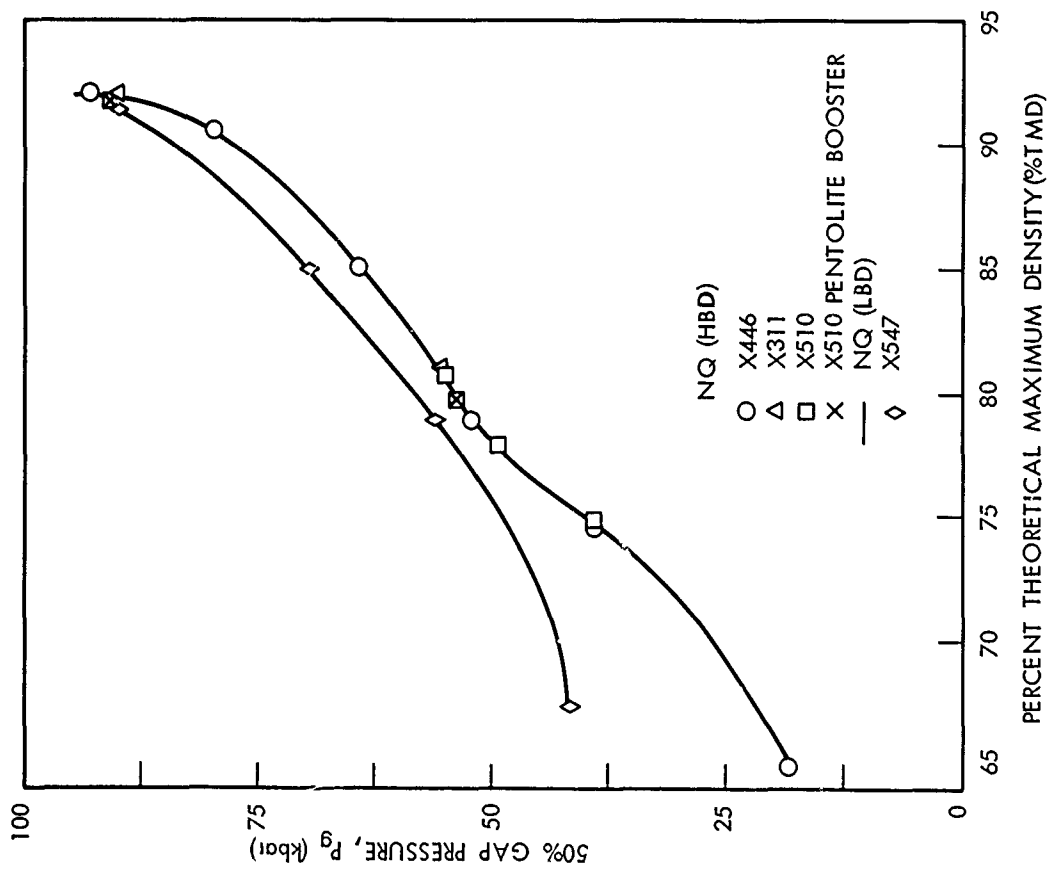


FIG. 13 SHOCK SENSITIVITY CURVES FOR HIGH AND LOW BULK DENSITY NQ

NOLTR 67-169

TABLE 12

MOST RECENT SHOCK SENSITIVITY TESTS ON NQ

<u>NQ</u>	<u>ρ_0</u> <u>g/cc</u>	TMD <u>%</u>	<u>50% Point</u>	
			<u>No.</u> <u>Cards</u>	<u>P</u> <u>g</u> <u>(kbar)</u>
X589	1.4371	80.7	80	58
	1.4391	80.8	79	58.5
	1.5161	85.1	68	65
	1.3881	78.0	97.5	50
X588	1.3871	78.0	109	46
	1.4401	81.0	98	50
	1.5041	84.5	81	57.5

there was a decided peculiarity in the shock sensitivity curve (same qualitative direction as that of Fig. 13), and there was an apparent reversal in sensitivity ratings of the fine and coarse tetryl when the small rather than the large scale test results were used. The close parallelism with the behavior of NQ¹ coupled with the Ref. 17 results: (a) that tetryl (400 - 630 μ) exhibits LVD and (b) that at $\rho_0 = 0.9$ g/cc, its d_c value is about 12 mm, i.e., approximately the gap test diameter used in Ref. 21, make it possible to explain these tetryl results in the same way as those for NQ.

SUMMARY

Recent detonation velocity data for NQ at high (1.7 g/cc) and low ρ_0 lie on the currently used ideal curve down to $\rho_0 \sim 0.3$ g/cc. Below this density the velocities lie above the straight line and appear to vary slowly with density to the terminal value of 2.05 mm/ μ sec computed for $\rho_0 = 0.01$ g/cc.

Work with NQ (LBD) showed that the diameter effect on D is small for this material, particularly at high densities. Its failure curve and detonation velocity pattern were typical of Group 1 explosives.

The high bulk density NQ also showed Group 1 behavior in the density range of 1.3 to 1.6 g/cc ($d \geq 5.08$ cm), coupled with failures to initiate at $\rho_0 > 1.62$ g/cc (dead pressing). However, NQ (HBD) exhibited diameter- and density-dependent pseudo-detonations (LVD) in the density range of 0.7 to 1.1 g/cc. The functional relation between LVD, ρ_0 , and d differs markedly from that of D, ρ_0 , and d. In addition, the limit curve for d and ρ_0 in LVD shows the opposite trend to that of the failure curve in detonation, i.e., it shows that the critical density for LVD increases with increasing diameter.

It is to the existence of this LVD region that a previously unexplained hump in the shock sensitivity curve of NQ (HBD) is now attributed. [Although the LVD is of lower velocity than detonation, its driving reaction is frequently sufficiently powerful to damage

NOLTR 67-169

the steel witness used in the gap test.] Grinding NQ (HBD) to a finer material (and hence decreasing its critical diameter for detonation) resulted in a shock sensitivity curve showing no hump (Fig.14).

ACKNOWLEDGEMENT

The authors wish to thank many colleagues who assisted in this work. In particular, G. Roberson, I. Jaffe, D. Edwards, and J. O. Erkman have each contributed to various parts of the study. C. Lyttle of the Chemical Engineering Division cooperated closely with us in preparing the charges; and the personnel of NOS, in preparing NQ Batch X588.

REFERENCES

1. D. Price and T. P Liddiard, Jr., "The Small Scale Gap Test: Calibration and Comparison with the Large Scale Gap Test", NOLTR 66-87 (7 July 1966).
2. D. Price, "Contrasting Patterns in the Behavior of High Explosives", Eleventh Symposium (International) on Combustion, The Combustion Institute, Pittsburgh (1967), pp 693-702.
3. V. Milani, R. Evans, S. Skolnik, and F. C. Thames, "The Preparation of High Bulk Density Nitroguanidine", NAVORD Report 3037 (Dec. 1953)
4. A. R. Clairmont, Jr., I. Jaffe, and D. Price, "The Detonation Behavior of Ammonium Perchlorate as a Function of Charge Density and Diameter", NOLTR 67-71, (20 Jun 1967)
5. A. R. Clairmont, Jr. and I. Jaffe, "Analysis of Optical Determination of Detonation Velocity in Short Charges", S.P.I.E. Journal 5, 18-21 (1966). See also NOLTR 64-23.
6. H. Heller, O. H. Johnson, and J. M. Rosen, NAVORD 6688 (1959). Confidential
7. "Properties of Chemical Explosives", UCRL-14592, Univ. of California, Lawrence Radiation Lab., Livermore, Calif. (1965).
8. M. D. Hurwitz, OSRD 5611 (1945).
9. "Military Explosives", TM 9-1910 and TO 11A-1-34, Depts. of the Army and the Air Force (1955).
10. W. B. Benedick, Rev. Sci. Instru. 36, 1309-15 (1965). See also Sandia Research Report, SC-4967(RR), (1963).

NOLTR 67-169

11. J. Savitt, "New Explosives Evaluation Techniques", Tech. Doc. Rept. ATL-TDR-64-16, Eglin AF Base (1964). Confidential
12. W. B. Benedick, private communication.
13. L. N. Stesik and N. S. Shvedova, PMTF (1964) pp 124-126. Translated by LCDR W. W. Bannister. ONI Translation No. 2111.
14. V. K. Bobolev, Dokl. Akad. Nauk SSSR 57, 789 (1947). Translated by U. S. Joint Publications Res. Service, JPRS: 4026.
15. S. Paterson cited in J. Taylor, "Detonation in Condensed Explosives", Clarendon Press, Oxford (1952) p 163 et seq.
16. E. Jones and D. Mitchell, "Spread of Detonation in High Explosives", Nature 161, 98-99 (1948).
17. A. K. Parfenov and A. Ya. Apin, "Low Velocity Detonation in Pulverized Explosives", Scientific and Technical Problems of Combustion and Explosion (No. 1, 1965), pp 151-55, U. S. Dept. of Commerce JPRS 32,529, TT 65-33008.
18. O. A. J. Gurton, "The Role of Gas Pockets in the Propagation of Low Velocity Detonation", Preprints Second ONR Symposium on Detonation (1955).
19. F. P. Bowden, "The Initiation and Growth of Explosion in the Condensed Phase", Ninth Symposium (International) on Combustion, Academic Press, New York (1963) pp 499-516.
20. I. Jaffe, G. E. Roberson, A. R. Clairmont, Jr., and D. Price, "The NOL Large Scale Gap Test. Compilation of Data for Propellants and Explosives II", NOLTR 65-177, (15 Nov 1965) Confidential
21. L. B. Seely, "A Proposed Mechanism for Shock Initiation of Low Density Granular Explosives", Proceedings of Fourth Electric Initiator Symposium at Franklin Institute, Phila. 1963 Paper 27 of Rept. EIS-A2357.

APPENDIX A

ADDITIONAL INFORMATION ON THE LOTS OF NQ USED

Sieve analysis is inappropriate for fine materials of high t/d such as the NQ (LBD). As remarked in the text, X547 was in the form of hollow needle-like crystals. A typical photomicrograph appears in Ref 10.

The Ro-Tap Sieve Analyser was used for the NQ (HBD) although, as the results show, this is not an ideal method of gaging grain size. Table A1 contains the data which show 50% weight median values of 106, 95, and 117 μ for lots X530, 589, and 588, respectively. It seems highly unlikely that X538 (ground X589) is actually coarser than X589. Figs A1-3 are photomicrographs of X588 showing the large amount of fine material ($< 10 \mu$); the coarse material is comparable to that of the original, unground NQ. Moreover, X588 detonates as a finer material than either X589 or X530, and X530 as finer than X589, but in both cases screen analysis indicated the reverse in relative fineness. Factors such as an unfavorable t/d and electrostatic retention of fines are evidently distorting the mean size as determined by the Ro-Tap. Under these circumstances, there seemed little point in running additional sieve analyses.

TABLE A1
RO-TAP SIEVE ANALYSES ON NQ (HBD)

Material	Sample (100g)	% on sieve No.:	149	105	74	62	53	44	<44	:Mesh(μ) Total	Median size, μ
			100	140	200	230	270	325	Pan		
X510	1	% < d:	23.6	25.5	17.0	7.6	7.0	4.0	12.2	96.9	100
			76.4	50.9	33.9	26.3	19.3	15.3	--		
X530	1		26.3	25.2	17.1	7.6	7.1	4.0	12.2	99.5	
	2	AV	23.7	25.8	17.0	7.5	7.0	4.1	12.1	97.2	
		% < d:	25.0	25.5	17.0	7.6	7.0	4.0	12.2	98.3	106
X589	1		75.0	49.5	32.5	24.9	17.9	13.9	--		
	2	AV	19.5	22.5	18.8	15.2	8.7	5.0	10.2	99.9	
		% < d:	29.5	18.1	18.9	9.2	8.1	5.8	9.4	99.0	95
X588 (X589 ground)	1		24.5	20.3	18.8	12.2	8.4	5.4	9.8	99.4	
	2	AV	75.5	55.2	36.4	24.2	15.8	10.4	--		
		% < d:	25.7	22.9	19.1	7.9	7.4	5.8	11.0	99.8	
			48.4	17.9	14.0	5.5	5.3	2.3	6.0	99.4	
			37.0	20.4	16.6	6.7	6.4	4.0	8.5	99.6	
		AV	63.0	42.6	26.0	19.3	12.9	8.9	--		117
		% < d:									

NOLTR.67-169



FIG. A-1 PHOTOMICROGRAPHS OF NQ (X588)

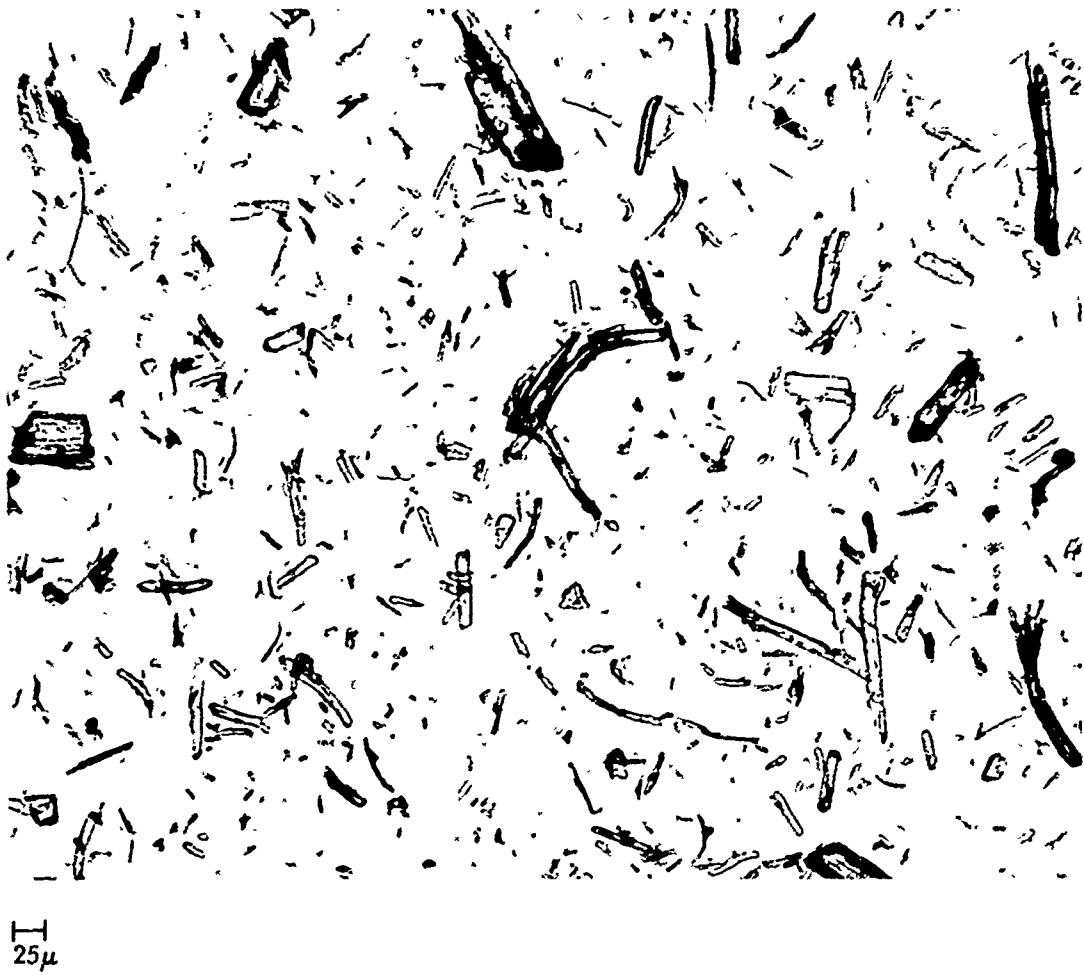


FIG. A-2 PHOTOMICROGRAPHS OF NQ (X588)

NOLTR 67-169

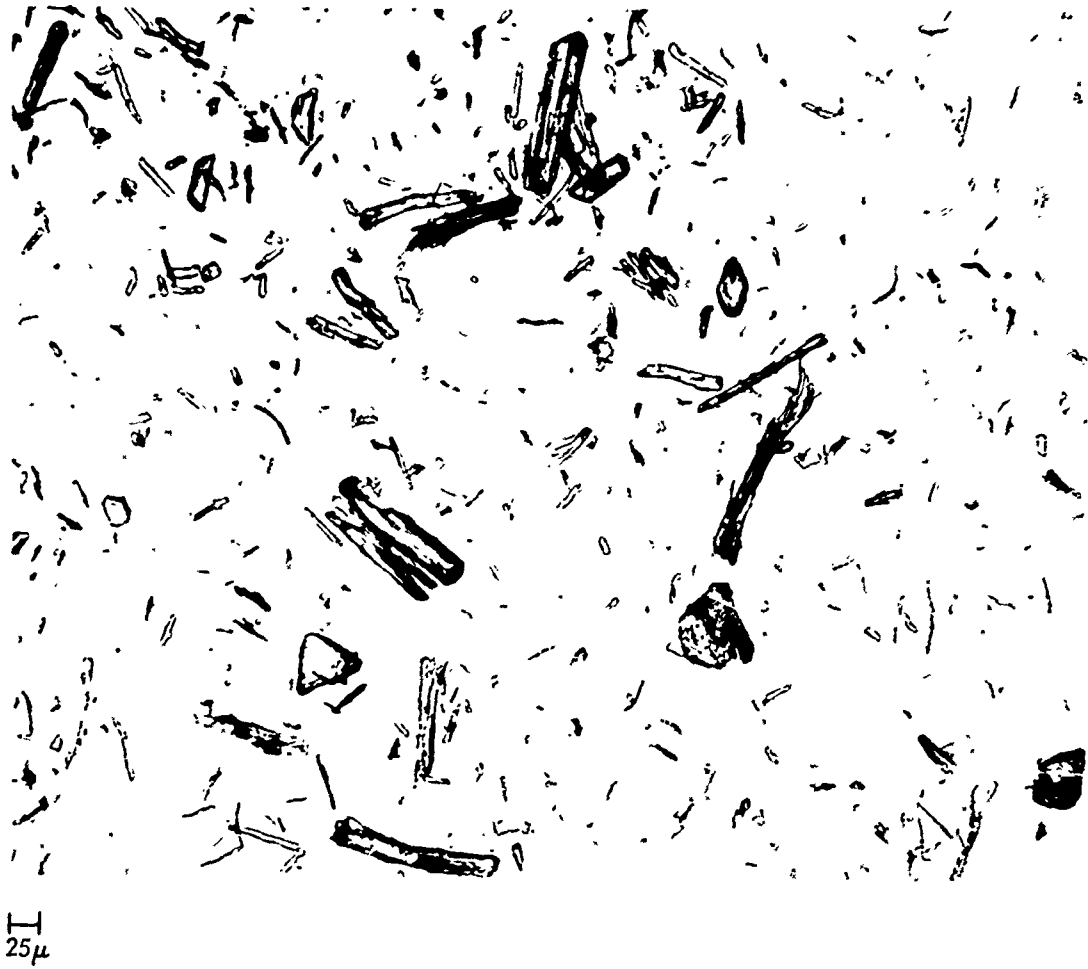


FIG. A-3 PHOTOMICROGRAPHS OF NQ (X588)

APPENDIX B

SUPPLEMENTARY DATA

Table B1 contains the optical details for each of the 70 mm smear camera records obtained. Table B2 contains the velocities obtained by fitting the position-time (x-t) data to the various functions:

- (a) linear
- (b) hyperbolic (contains cross product xt)
- (c) quadratic
- (d) Spline fit (sequential cubic segments, continuous first and second derivatives.)

Whenever such a fit is made, the overall velocity for the interval can be found. The linear fit (a) has been used for all velocities reported in the tables of the text of this report. As Table B2 shows, from the sampling so far made, the overall velocity from the spline fits agrees very well with the velocity from (a) although there is no question that the spline treatment seems to give the best fit of the four to the actual x-t data.

In deciding whether the measured velocity is constant over the 63.5mm interval chosen near the end of the charge, we need some way of estimating the departure of the smear trace from a straight line. We have found by working with straight edges that variables in the record reading and reducing procedures can introduce as much as 2% change in the velocity. We can compute that our use of a curved initiating shock will introduce up to 1% velocity change at the largest diameter (7.62 cm). Various other factors such as roughness and heterogeneity of the charge surface, over- or underexposure of the film, and stability of the front itself have effects that we have not yet been able to assess. It should be noted that for most of the shots in Table B2, the camera viewed the last six inches of the charge because the response (constant or attenuating velocity) was unknown. Consequently the time resolution is only about half

that attainable when a length only 2.5 in. of charge is viewed; 2.5 in. is used whenever a constant velocity front is expected. The poorer time resolution (6 in. view) very probably contributes something to the larger percentage changes observed. The absolute value of the change as well as its percentage value must also be kept in mind; random errors would be expected to show larger percentage effects at the lower velocities.

Again from the sampling, methods (b) and (c) generally measure about the same percentage change. The decision as to whether this indicates constancy or failure is still subjective. Up to 3% variation can be accounted for. Thus shot 305 (14%) is undoubtedly failing, shots 310 and 318 (2.7-3.2%) probably detonating, and shot 279 (6%) is also considered a detonation because of its location in the D vs ρ_0 family of curves in Fig. 8. It is possible that the factor of 2 difference in the velocity change for shot 279 as compared to shots 310 and 318 could arise because the latter two charges were prepared hydrostatically and consisted of four two-inch long pellets whose camera smear records are consequently made up of four arcs instead of the single one from the isostatically pressed charge No. 279. Moreover, the longitudinal density variation and hence detonation velocity would differ within the charges prepared in the different presses. Finally, any charge near its failure limit would be expected to show more instability of its front than a definitely super-critical charge.

In the low velocity regime, we are faced with both the lower absolute values of U_{LV} and the metastability of the disturbance. The latter fact means that propagation of the low velocity front will be much more sensitive to charge heterogeneity than would a detonation. Again our decision of constancy or failure has to be made, in part, from the U_{LV} pattern of Fig. 10. Thus because of the respective locations, Shot 288 (7.2%) is more apt to be a constant velocity than Shot 289 (4.4%). It is evident from the velocity changes shown in Table B2 that low ρ_0 and low d both

enhance the possibility of U_{LV} . The exact point at which ρ_0 and d have increased to the extent that this particular NQ(HBD) no longer exhibits a metastable reaction, but an unquestionably unstable one, cannot be selected without doing much more work on longer charges. The large values of some of the velocity changes (Table B2) suggest that some of the U_{LV} shown at higher ρ_0 and d in Fig. 10 are in fact attenuating shocks; if so, the limit curve of Fig. 12 should be shifted to the left. On the other hand, the change in velocity found for the more dubious cases is comparable to that found in detonation near the critical density (Shot 279); this suggests that the figures as now shown are correct.

The important result of the present work is the demonstration of the existence of an extensive low velocity region, not the exact boundaries of this region in the d - ρ_0 plane. For reasons discussed above, these boundaries would be very difficult to establish, would be of no theoretical interest, and would be almost impossible to verify (reproduction of a failure limit of a metastable phenomenon). Consequently, no further work on this topic is planned.

TABLE B1
EXPERIMENTAL CONDITIONS FOR THE SHOTS

Shot No.	Flasher a	Length Observed in.	Writing Speed mm/ μ sec	Shot No.	Flasher a	Length Observed in.	Writing Speed mm/ μ sec
77*		7.5	4	326		6	2
78*		7.5	1	327	N	6	2
79*		7.5	1	328	N	6	2
102*	N	7.5	1				
103*	N	2.5	3	276		6	2
105*	N	2.5	3	291*		6	2
106*	Lacquer	2.5	3				
107*	N	2.5	3	277		6	2
80*	S	5	4	292*		6	2
81*	S	5	4	306		6	2
240		6	2	316		6	2
422*		6	2	293*		6	2
242		6	2	305	N	6	2
133	M	7.5	2	310	N	6	2
138	M	7.5	1	330	N	6	2
241	N	6	2	318	N	6	2
184	N	7.5	2	279	N	6	2
159	M	7.5	2	317	N	6	2
213	M	7.5	2	282	N	6	2
215	M	7.5	2	304	N	6	2
162	M	7.5	1	281	M	6	2
175	N	7.5	2	273	M	6	2
176	N	7.5	2	280	M	6	2
214	M	7.5	2	294	M	6	2
216	M	7.5	2	303	M	6	2
157	M	7.5	2	309	M	6	2
163	M	7.5	2	268		6	1
				270		2.5	2
				288		6	3

TABLE B1 (Con't)

Shot No.	Flasher a	Length Observed in.	Writing Speed mm/μsec	Shot No.	Flasher a	Length Observed in.	Writing Speed mm/μsec
269		2.5	2	262		2.5	2
266		6	1	257		6	2
289		6	2	258		6	2
290	N	6	2	247		7.5	2
325	N	6	2	244	M	6	2
267	M	6	3	245	M	7.5	2
265	N	6	2	243	M	6	2
329	N	6	2				
331	N	6	2	397		6	2
314	N	6	2	396	N	6	2
311	N	6	2	395	N	6	3
312	M	6	2	399	N	2.5	4
271	M	4	2				
315	M	6	2	411		2.5	4
				410	N	2.5	4
313	M	6	2	409	N	2.5	4
260		6	1				
264		2.5	2				
308		6	1				
259		6	1				
263		2.5	2				
307		6	1				
251	N	7.5	1				
254	M	7.5	1				
249	M	7.5	1				
250	M	7.5	1				
255		7.5	1				
252		7.5	1				
248		7.5	1				
253		7.5	1				
256		6	1				
261		2.5	2				

a. Cellulose acetate used unless otherwise specified. Symbols are: M Magic Tape, N none, S Scotch tape.

* Panatomic-X film used here; Tri-X film was used in remaining shots

TABLE B2
RESULTS OF VARIOUS TREATMENT OF x-t DATA

Shot No.*	d cm	ρ_0	U _{LV} (mm/usec)		% Change**		
			Linear Fit#	Hyper. Fit	Spline	Quad.	Hyper.
264	2.54	0.72	2.349	2.349	2.357	+3.1	-0.4
263	2.54	1.001	2.500			-0.1	--
268	3.81	0.735	2.942	2.959	2.949	+1.2	+1.1
270	3.81	0.735	2.874	2.873	2.841	+0.1	0.0
288	3.81	0.851	3.188	3.068	3.174	-6.9	-7.2
289	3.81	1.101	3.109	3.038	3.092	-4.4	-4.4
276	5.08	0.718	3.211	3.212	3.213	+2.4	-0.0
291	5.08	0.851	3.554	3.492	3.552	-5.3	-6.4
277	5.08	1.001	3.735			-7.6	--
293	5.08	1.102	3.784			-7.0	--
Detonating or Failing Near Critical Density							
305	5.08	1.200H	F(4.88)			-14.0	
310	5.08	1.251H	5.579			-2.7	
318	5.08	1.291H	6.125			-3.2	
279	5.08	1.2991	6.518			-6.0	

* Length of charge observed by camera was 2.5 in. for shots 263, 264, and 270; for all other shots, this length was 6 in.

** Change in U_{LV} over the portion of smear record which was read; this portion of the record corresponds to the last 63.5 mm of the charge.

UNCLASSIFIED

Security Classification

DOCUMENT CONTROL DATA - R&D		
<i>(Security classification of title, body of abstract and indexing annotation must be entered when the overall report is classified)</i>		
1. ORIGINATING ACTIVITY <i>(Corporate author)</i> U. S. Naval Ordnance Laboratory White Oak, Silver Spring, Maryland 20910		2a. REPORT SECURITY CLASSIFICATION UNCLASSIFIED
		2b. GROUP
3. REPORT TITLE THE RESPONSE OF NITROGUANIDINE TO A STRONG SHOCK		
4. DESCRIPTIVE NOTES <i>(Type of report and inclusive dates)</i>		
5. AUTHOR(S) <i>(Last name, first name, initial)</i> Donna Price and A. R. Clairmont, Jr.		
6. REPORT DATE 2 February 1968	7a. TOTAL NO. OF PAGES	7b. NO. OF REFS 21
8a. CONTRACT OR GRANT NO.	9a. ORIGINATOR'S REPORT NUMBER(S) NOLTR 67-169	
b. PROJECT NO. ORD Task 033 102 F009 06 01	9b. OTHER REPORT NO(S) <i>(Any other numbers that may be assigned this report)</i>	
c.		
d.		
10. AVAILABILITY/LIMITATION NOTICES This document is subject to special export controls and each transmittal to foreign governments may be made only with prior approval of NOL		
11. SUPPLEMENTARY NOTES	12. SPONSORING MILITARY ACTIVITY Naval Ordnance Systems Command	
13. ABSTRACT In its range of detonability, nitroguanidine (NQ) behaves as a Group 1 explosive. In addition, it exhibits failure at the high TMD ($> 94\%$ at 5.08 cm diam) as well as the more common failure at a lower critical density. The high bulk density (HBD) form of NQ exhibits a critical diameter about three times that of the low bulk density form. This fact aided in studying the subcritical region of NQ (HBD) where a strong shock produces a subdetonation, supersonic, constant velocity front. This pseudo-detonation or LVD had failure characteristics similar to the detonability limits of Group 2 materials. That trend, the power of the LVD reactions, and the dimensions of the various gap tests can be combined to explain (1) a hump in the curve 50% pressure vs % TMD obtained for NQ(HBD) in the gap test and (2) a reversal in <u>apparent</u> shock sensitivity rating of NQ(HBD) and NQ(LBD) when tested on the large- and small-scale gap tests. /		

DD FORM 1473
1 JAN 64

Security Classification

Security Classification

14. KEY WORDS	LINK A		LINK B		LINK C	
	ROLE	WT	ROLE	WT	ROLE	WT
<p>Nitroguanidine</p> <p>High bulk density nitroguanidine</p> <p>Detonation Velocity</p> <p>Low velocity detonation</p> <p>Detonability</p> <p>Critical diameter</p> <p>Critical Density</p> <p>Shock Sensitivity</p>						

INSTRUCTIONS

1. **ORIGINATING ACTIVITY:** Enter the name and address of the contractor, subcontractor, grantee, Department of Defense activity or other organization (*corporate author*) issuing the report.
- 2a. **REPORT SECURITY CLASSIFICATION:** Enter the overall security classification of the report. Indicate whether "Restricted Data" is included. Marking is to be in accordance with appropriate security regulations.
- 2b. **GROUP:** Automatic downgrading is specified in DoD Directive 5200.10 and Armed Forces Industrial Manual. Enter the group number. Also, when applicable, show that optional markings have been used for Group 3 and Group 4 as authorized.
3. **REPORT TITLE:** Enter the complete report title in all capital letters. Titles in all cases should be unclassified. If a meaningful title cannot be selected without classification, show title classification in all capitals in parenthesis immediately following the title.
4. **DESCRIPTIVE NOTES:** If appropriate, enter the type of report, e.g., interim, progress, summary, annual, or final. Give the inclusive dates when a specific reporting period is covered.
5. **AUTHOR(S):** Enter the name(s) of author(s) as shown on or in the report. Enter last name, first name, middle initial. If military, show rank and branch of service. The name of the principal author is an absolute minimum requirement.
6. **REPORT DATE:** Enter the date of the report as day, month, year; or month, year. If more than one date appears on the report, use date of publication.
- 7a. **TOTAL NUMBER OF PAGES:** The total page count should follow normal pagination procedures, i.e., enter the number of pages containing information.
- 7b. **NUMBER OF REFERENCES:** Enter the total number of references cited in the report.
- 8a. **CONTRACT OR GRANT NUMBER:** If appropriate, enter the applicable number of the contract or grant under which the report was written.
- 8b, 8c, & 8d. **PROJECT NUMBER:** Enter the appropriate military department identification, such as project number, subproject number, system numbers, task number, etc.
- 9a. **ORIGINATOR'S REPORT NUMBER(S):** Enter the official report number by which the document will be identified and controlled by the originating activity. This number must be unique to this report.
- 9b. **OTHER REPORT NUMBER(S):** If the report has been assigned any other report numbers (*either by the originator or by the sponsor*), also enter this number(s).
10. **AVAILABILITY/LIMITATION NOTICES:** Enter any limitations on further dissemination of the report, other than those

imposed by security classification, using standard statements such as:

- (1) "Qualified requesters may obtain copies of this report from DDC."
- (2) "Foreign announcement and dissemination of this report by DDC is not authorized."
- (3) "U. S. Government agencies may obtain copies of this report directly from DDC. Other qualified DDC users shall request through _____."
- (4) "U. S. military agencies may obtain copies of this report directly from DDC. Other qualified users shall request through _____."
- (5) "All distribution of this report is controlled. Qualified DDC users shall request through _____."

If the report has been furnished to the Office of Technical Services, Department of Commerce, for sale to the public, indicate this fact and enter the price, if known.

11. **SUPPLEMENTARY NOTES:** Use for additional explanatory notes.
12. **SPONSORING MILITARY ACTIVITY:** Enter the name of the departmental project office or laboratory sponsoring (*paying for*) the research and development. Include address.
13. **ABSTRACT:** Enter an abstract giving a brief and factual summary of the document indicative of the report, even though it may also appear elsewhere in the body of the technical report. If additional space is required, a continuation sheet shall be attached.

It is highly desirable that the abstract of classified reports be unclassified. Each paragraph of the abstract shall end with an indication of the military security classification of the information in the paragraph, represented as (TS), (S), (C), or (U).

There is no limitation on the length of the abstract. However, the suggested length is from 150 to 225 words.

14. **KEY WORDS:** Key words are technically meaningful terms or short phrases that characterize a report and may be used as index entries for cataloging the report. Key words must be selected so that no security classification is required. Identifiers, such as equipment model designation, trade name, military project code name, geographic location, may be used as key words but will be followed by an indication of technical context. The assignment of links, roles, and weights is optional.